From ultra to nanofiltration: a review on the fabrication of ZrO2 membranes

Bortot Coelho, Fabrício E.; Magnacca, Giuliana; Boffa, Vittorio; Candelario, Victor M.; Luiten-Olieman, Mieke; Zhang, Wenijng

Published in:
Ceramics International

DOI (link to publication from Publisher):
10.1016/j.ceramint.2023.01.076

Publication date:
2023

Document Version
Publisher's PDF, also known as Version of record

Ceramics International 49 (2023) 8683–8708

Contents lists available at ScienceDirect

Ceramics International

journal homepage: www.elsevier.com/locate/ceramint

Review article

From ultra to nanofiltration: A review on the fabrication of ZrO_2 membranes

Fabricio Eduardo Bortot Coelho [a,d,*], Giuliana Magnacca [b], Vittorio Boffa [c], Victor M. Candelario [d], Mieke Luiten-Olieman [e], Wenjing Zhang [a]

[a] Department of Environmental and Resource Engineering, Technical University of Denmark, Miljøvej 113, 2800, Kongens Lyngby, Denmark
[b] Department of Chemistry and NIS Interdepartmental Centre, University of Turin, Via P. Giuria 7, 10125, Torino, Italy
[c] Department of Chemistry and Bioscience, Aalborg University, Fredrik Bajers Vej 7H, DK-9220, Aalborg Øst, Denmark
[d] Department of Research and Development, Liqtech International A/S, Industriparken 22 C, 2750, Ballerup, Denmark
[e] Inorganic Membranes, MESA+ Institute for Nanotechnology, University of Twente, PO Box 217, 7500, AE Enschede, the Netherlands

ARTICLE INFO

Handling Editor: Dr P. Vincenzini

Keywords:
Zirconia
ZrO_2
Ceramic membranes
Sol-gel
Membrane fabrication
Wastewater

ABSTRACT

Zirconia (ZrO_2) membranes experienced rapid progress in applications demanding high-stability membranes own to their higher chemical resistance and hydrophilicity compared to silica and alumina. Moreover, ZrO_2 membranes have increased fouling resistance, high permeability, and a long lifetime making them broadly applied in drinking water production, wastewater treatment, petrochemical, food, and beverages industries. However, fabricating ZrO_2 membranes for Nanofiltration and Gas Separation is still challenging. This paper reviews the progress in fabricating ZrO_2 membranes, focusing on strategies for achieving smaller pores without losing their high permeability and selectivity. The current state of the art in commercial ZrO_2 membranes and the recent innovations in academia are critically reviewed. A comprehensive revision of sol-gel technique's critical synthesis and process parameters is presented along with the most recent molecular layer deposition method. This work aims to provide a guide for both starting and established researchers, thus filling a gap in the present literature.

1. Introduction

Economic and scientific developments have brought welfare to humankind, increasing life expectancy and allowing populational growth. However, the rapid improvement of living standards raised the pressure on the environment [1]. The increasing water demand for extractive and transformation industries, as well as for agricultural and urban supply, is endangering the most precious resource on earth [2]. Furthermore, inappropriate disposal of wastewaters is bringing contaminants of emerging concern (CECs), such as pharmaceuticals, pesticides, flame-retardants, and antibiotics, to water streams [3,4]. In this context, the search for more sustainable production processes, water reuse, and more effective wastewater treatments led inevitably to the development of membrane technology.

Membrane filtration presents several advantages over traditional processes, such as high throughput, high retention of contaminants, continuous operation, easiness to scale up and to operate, small footprint, and higher energy efficiency [5–7]. Polymeric membranes currently dominate the market due to their low cost, good performance, and advanced stage of development [8,9]. However, their poor stability in harsh environments, easy fouling, and short lifetime can limit the application of polymeric membranes. On the contrary, ceramic membranes have several advantages compared to polymeric ones, including higher thermal, mechanical, and chemical stabilities; well-defined pore size distribution; higher hydrophilicity; longer membrane lifetimes; high fluxes at low pressures; higher porosity; and lower fouling tendency [10–12]. In addition, ceramic membranes are resistant to organic solvents and provide higher fluxes than polymeric ones owing to their mechanical stability under elevated pressure gradients [13]. Therefore, ceramic membranes are usually applied in operating conditions in which polymeric membranes are unsuitable, such as high temperatures, heavily contaminated or radioactive feeds, and aggressive solvents [14].

On the other hand, the fabrication of these membranes may be complex and involve high manufacturing costs [2]. Despite their outstanding properties, most of the commercialised ceramic membranes are for microfiltration (MF) and ultrafiltration (UF) [2,10,15]. In this

* Corresponding author. Department of Environmental Engineering, Technical University of Denmark, Miljøvej 113, 2800, Kongens Lyngby, Denmark.
E-mail address: feabfc@gmail.com (F.E. Bortot Coelho).

https://doi.org/10.1016/j.ceramint.2023.01.076
Received 29 November 2022; Received in revised form 9 January 2023; Accepted 10 January 2023
Available online 14 January 2023

context, in the past years, great attention has been devoted to developing ceramic membranes with nanometric and sub-nanometric pore sizes to increase their use in nanofiltration (NF), pervaporation, and gas separation [16].

The most common materials applied in membrane fabrication (Table 1) are silica (silicon dioxide - SiO_2), alumina (aluminium oxide - Al_2O_3), zeolites, silicon carbide (SiC), titania (titanium dioxide - TiO_2), and zirconia (zirconium dioxide - ZrO_2) [17]. Alumina (together with silica and zeolite) membranes have been dominant in the market [10], considering these materials' cost-effectiveness and well-stabilised fabrication techniques [18]. However, the insufficient chemical and thermal stability of SiO_2 and γ-Al_2O_3 under corrosive and aggressive conditions such as pH < 3, pH > 10, and hydrothermal environments (300 °C, 15 bar) [19–21] can limit the application of these membranes in harsh conditions [22]. For example, Hofs et al. [11] reported a reduction in the transmembrane pressure during lake water filtration due to the dissolution of the SiO_2 membrane utilised.

On the contrary, SiC, TiO_2, and ZrO_2 present extremely high chemical stabilities, making these materials stable in almost all pH ranges. In Fig. 1, the properties of the membranes fabricated with different oxides (Al_2O_3, TiO_2, and ZrO_2) and non-oxide (SiC) are compared. Even though silicon carbide seems more appropriate than zirconia for membrane fabrication, its sintering requires much higher temperatures in an inert atmosphere, making SiC much more expensive than ZrO_2 [23,27,30,32]. Moreover, the development of microporous SiC membranes is still in an early stage due to the complexity of the layer formation and sintering process [27,32]. The reported SiC membranes are still in the ultrafiltration range [27,29].

Therefore, zirconia is the most promising material for developing high-resistance and high-flux microporous ceramic membranes. In addition, ZrO_2 presents higher corrosion resistance than TiO_2 [33], especially in strong alkaline media [13], where also silica and alumina membranes fail [34]. Own to zirconia refractory properties and elevated mechanical strength, it can work at high temperatures [35] and under high pressures [36].

For those reasons, there is an increasing interest in the fabrication of ZrO_2 membranes, as shown by the publication trend in Fig. 2a. Indeed, after the 2000s, there was an exponential growth in the number of papers published about zirconia membranes, reaching almost 700 works reported from 2016 to 2021.

Several of those works demonstrate the relevance and importance of zirconia membranes by applying commercial or newly developed membranes in industrial settings or in innovative applications. Table 2 summarize the main applications of zirconia membranes giving some of the most remarkable examples. For each one, the geometry, type, pore size and permeability of the membrane tested are presented together with the most relevant results obtained. Owe to ZrO_2 membranes' chemical, thermal, and mechanical stabilities, zirconia membranes are applied majorly in conditions that require stable and high-performing membranes to filter heavily contaminated or corrosive feeds such as in wastewater treatment [31,39–50], organic solvent filtration [51–53], drinking/surface waters filtration [11,54–59] radioactive waste filtration [60], pre-treatment for RO [61], Desalination [62–65], and gas separation/pervaporation [66,67]. Moreover, the super hydrophilicity, high fluxes at low pressures, and lower fouling tendency of zirconia membranes [10–12] led to excellent results in oil/water separation (oily wastewater treatment) [68–76] and in applications requiring operation under high pressures, severe backwashing, cleaning, and disinfection steps [14,31,36,37] such as pharmaceutical, food, beverages, and dairy industries [77–86].

Some applications of ZrO_2 membranes have been hot topics in the scientific community recently, such as the removal of microplastics [46], high-temperature wastewater treatment [31,43,47], recovery and concentration of silver nanoparticles [87], water disinfection by retention of virus and bacteria [58,59], micropollutants (*e.g.* pesticides, pharmaceuticals) removal [41], and recovery of valuable biomolecules

Table 1
Advantages and drawbacks of commonly applied materials in the fabrication of ceramic membranes.

Material	Advantages	Disadvantages	Reference
Alumina (Al_2O_3)	- The most common raw material for the fabrication of ceramic membranes. - Good chemical and thermalstabilities. - Established methods for MF, UF, and NF membranes fabrication - Due to its easy processing and intrinsic properties of high strength and good chemical and thermal stability, alumina can function as a substrate, intermediate, and active layer in a ceramic membrane.	- High sintering temperatures (>1300 °C). - Low stability in acid (pH < 3) and alkaline (pH > 10) media. - High fouling tendency. - Lower chemical resistance than TiO_2, ZrO_2, and SiC.	[2,23]
Silica (SiO_2)	- The 2nd most used material for ceramic membranes. - Easiness of controlling pore size makes it a common material for molecular sieving and gas separation - Stability can be improved by mixing with Al2O3 and ZrO2.	- Soluble in low and high pH values - Unstable in hydrothermal conditions. - Shrinkage of pores own to physisorption of water molecules.	[11,24]
Zeolite	- weak swelling capacity in water. - Natural/synthetic raw material with molecular sieving function. - Applicable as a self-standing or coated layer. - Higher thermal resistance compared to SiC and Al_2O_3.	- Lower fluxes. - Higher thickness necessary to obtain a defect-free layer.	[23,25,26]
Silicon carbide (SiC)	- High chemical resistance (pH range for operation: 0–14). - High-temperature tolerance: up to 800 °C. - High operating pressure of up to 10 bar.	-High sintering temperature (>1800 °C). -High cost and complex fabrication. -Limitation on membrane pore size: commercial membranes are for MF. -The development of microporous membranes is still in an early stage.	[27–29]
Titania (TiO_2)	- Lower sintering temperature. - Photocatalytic functions. - High chemical resistance. - Applied for NF membrane manufacture.	- Anatase-rutile phase transformation can cause membrane cracking. - High reactivity of Ti-alkoxides. - Low surface area.	[20,23,30]
Zirconia (ZrO_2)	- Highest hydrophilicity and the biggest thermal resistance of oxidic ceramic membranes. - Elevated hardness. - Hydrothermal resistance.	- Monoclinic-tetragonal phase transformation can cause membrane cracking. - High reactivity of Zr-alkoxides.	[2,11,31]

(*continued on next page*)

Table 1 (*continued*)

Material	Advantages	Disadvantages	Reference
	- High chemical resistance (can operate with strong acidic or alkaline feeds, pH 0–14). - High operating pressure of up to 10 bar.		

from renewable sources [79]. It is worth noticing in Table 2 some remarkable results obtained with zirconia membranes, such as higher water permeability and less fouling than similar polymeric membranes [11,31,47,49], better restoration of the initial water permeability after cleaning [48], corrosion resistance in highly acid and alkaline media [73,84], and extended membrane lifetime to more than 8 years [76,82].

Besides zirconia's advantageous properties and potential applications, fabricating membranes with this material presents some challenges that hinder the development of such devices, *e.g.*, an unfavourable layer formation and the difficulty in obtaining small pores [88]. As shown in Fig. 2b, most works published about ZrO_2 membranes deal with UF and MF, but in the past decades, there has been a significant development in nanofiltration ZrO_2 membranes. Although some of these works led to commercial UF and NF zirconia membranes, there are still a few companies in this business, as presented in Table 3. This table summarizes the commercial ceramic membranes in which the separation/top layer is made of zirconia or mixed oxide-zirconia. Unfortunately, manufacturers did not disclose the exact membrane composition, crystal phase, top layer thickness, and water permeability. It should be noticed that these companies provide the nominal pore size, which can be quite different from the actual size [11].

One of the main challenges faced in the fabrication of ZrO_2 membranes is avoiding cracks in the top layer, which can be related to the change in the crystalline phases of the zirconia layer. To avoid cracks, the tetragonal or cubic polymorphs are usually fully or partially stabilised by doping zirconia with yttria. This material, yttria-stabilised zirconia (YSZ), is suitable for filtration membranes working under severe conditions (high temperatures, high pressures, and corrosive media), such as gas separation [100], pervaporation [101], organic solvent filtration [102], and highly acidic or basic feeds [103].

This review focuses on the fabrication of asymmetric membranes composed of a porous ceramic support (*e.g.,* zirconia, alumina, silicon carbide) with an intermediate or top layer made of zirconia or its mixtures with other oxides. Initially, an overview of the main achievements in membrane fabrication is presented in Section 2, followed by a detailed revision of the main fabrication technique, the sol-gel method, in Section 3, which discuses all the critical synthesis and process parameters. In Section 4, the background and prospects of most recent molecular layer deposition (MLD) method, which has been showing excellent results in obtaining microporous membranes, are briefly discussed.

2. Overview of the development of ZrO_2 membranes

To the best of our knowledge, one of the first works dedicated to sol-gel-derived ZrO_2 membranes was published in 1989 [104], a few years later than the development of microporous alumina membranes by sol-gel processes [105]. Since then, there has been significant progress not only in fabrication techniques but also in membrane

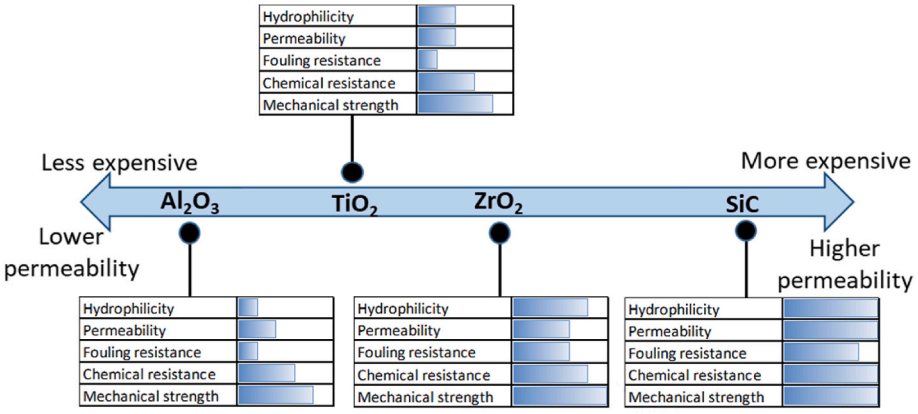

Fig. 1. Relative properties of ceramic membrane fabricated using alumina, titania, zirconia, and silicon carbide. Source: adapted from Refs. [30,38].

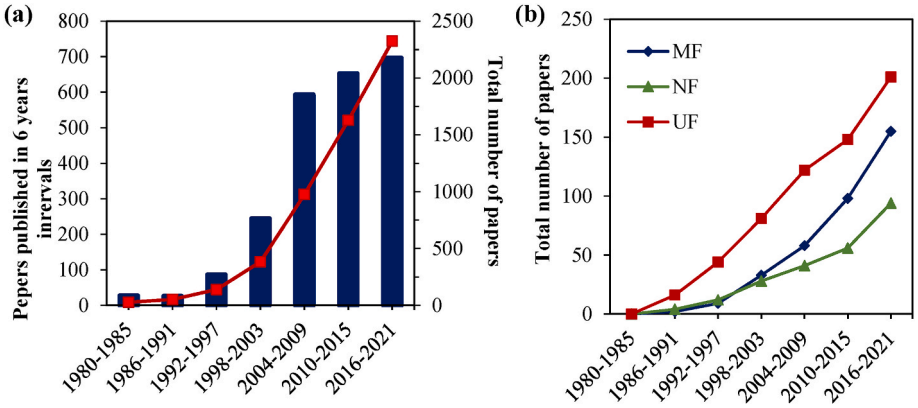

Fig. 2. Published papers concerning: (a) zirconia membranes and (b) MF, UF, or NF zirconia membranes. Source: Scopus® (Elsevier BV) database search: TITLE-ABS-KEY (zirconia AND membrane) OR TITLE-ABS-KEY (ZrO_2 AND membrane).

Table 2
Summary of the applications of ZrO_2 and mixed oxides-ZrO_2 membranes.

Application and Examples				
Membrane	Pore size (nm)	Permeability (LMH/bar)	Remarks	Reference
Wastewater treatment [31,39–50]				
Tubular UF–ZrO_2 on SiC support	60	350 (clean water) 275 (wastewater)	- Filtration of real wastewater from a washing cycle of industrial tents made from polyvinyl chloride (PVC) textile. - The MF membrane (SiC, 300 nm) manifested higher fouling and 95% permeability decrease compared to the UF membrane (ZrO_2, 60 nm), which presented 37% decrease. - 98.55% removal efficiency of microplastics from the laundry wastewater.	[46]
Tubular NF – 8YZS on Al_2O_3 support	1.4	28 (clean water) 8 (wastewater at 60 °C)	- Treatment of a dyeing process wastewater with a high content of a fluorescent brightener (245 g^{-1}, molecular weight = 1100 Da) and electrical conductivity 96,000 μS cm^{-1} and pH 9.4. - Retention of dye >98%. - Higher water permeability than that of the similar polymeric NF membranes. - Results indicate that ceramic NF membranes are promising in high-temperature dye wastewater treatment.	[31,47]
Tubular UF–ZrO_2 on Al_2O_3 support	100	200 (clean water) 25 (wastewater)	- UF of olive mill wastewater (OMWW) - Comparison between α-Al_2O_3 (0.1 μm), ZrO_2 (0.1 μm), and PVDF (0.3 μm) membranes. - Commercial MF/UF ZrO_2 membrane tested (TAMI Industries) - PVDF membranes were the least suitable for the treatment of OMWW due to both low permeate fluxes and irreversible fouling. - ZrO_2 membrane allowed the better restoration of the initial water permeability after cleaning.	[48]
Tubular UF–ZrO_2 on Al_2O_3 support	100–200	375 (clean water) 100 (wastewater)	- Waste emulsion from cold steel rolling mill (1–5% of oil) - Comparison of Al_2O_3 and ZrO_2 membranes: both had oil rejection >99.8%, but ZrO_2 membrane had 2x the water flux of Al_2O_3. - Comparison with polymeric membranes: ZrO_2 membrane had higher flux and less fouling.	[49]
Tubular - 20% TiO_2 : 80% ZrO_2 on Al_2O_3 support	1.4	10 (wastewater)	- Development of ZrO_2/TiO_2 mixed-oxide membranes.	[50]
Tubular - 90% TiO_2 : 10% ZrO_2 on Al_2O_3 support	1.7	40 (wastewater)	- Corrosion tests: Ti-rich membranes were corroded in strong acid (pH 0.2), while Zr-rich membranes were resistant. All mixed-oxide membranes were very resistant to strong bases. - Filtration of dye "Direct red": Zr-rich membrane has higher dye retention (98%) than Ti-rich membrane (96%)	
Flat-sheet MF – ZrO_2/TiO_2 on Al_2O_3 support	140	436 (clean water)	- Reactive photo-Fenton membrane coated with goethite (α-FeOOH). - Fouling test with bovine serum albumin (BSA) and humic acid (HA) - The combination of UV + $H2O_2$ + α-FeOOH led to the highest rates of foulant removal owing to the photo-Fenton reactions on the catalyst.	[40]
Disc NF – 8YSZ on Al_2O_3 support	1.4	4 (clean water)	- Treatment of pesticide wastewater by NF. – 89% of retention of the pesticide carbofuran. - The alkali wash and low-temperature calcination effectively cleaned the contaminated membranes to achieve multiple reuses.	[41]
Flat-sheet UF–ZrO_2/TiO_2 on SiC support	10	160 (clean water) 120 (wastewater)	- Photocatalytic membrane for treatment of an urban wastewater treatment plant (UWWTP) effluents. - Filtration significantly reduces the turbidity of the UWWTP effluent, increasing the degradation efficiency of the subsequent solar photo-Fenton treatment for CECs removal. - Under simulated solar-light irradiation, the membrane shows anti-fouling and self-cleaning properties.	[42]
Desalination [62–65]				
Flat sheet NF - YSZ on porous steel support	200–1000	380 (clean water)	- Membrane fabricated by plasma spraying - The membrane showed good fouling resistance, a superhydrophilic nature (contact Angle <10°). - Rejections of NaCl and methylene blue were higher than 99%	[63]
Tubular UF – Hydrophobic grafted ZrO_2	50	–	- Desalination by Direct Contact Membrane distillation (DCMD) - Comparison between ZrO_2 (50 nm) and TiO_2 (5 nm) membranes: ZrO_2 membrane provides the highest rejection rates and the best performance due to the lower resistance of water vapour transfer.	[64]
Tubular UF–ZrO_2	50	–	- Desalination by membrane distillation. - Al_2O_3 and ZrO_2 membranes with 200 and 50 nm pore diameters were grafted with fluoroalkylsilanes, making these membranes hydrophobic. - Only water vapour was transported through the membranes - The salt rejection in this process is close to 100%. - Commercial ZrO_2 membranes by Pall Exekia.	[65]
Oil/water separation [68–76]				
Tubular UF–ZrO_2 on Al_2O_3 support	50	220 (wastewater)	- Oil rejection: 99.9% - Cold-rolling emulsion wastewater treatment. - Commercial Membrane: Membralox® (Pall Corporation, USA). - Chemical oxygen demand (COD)removal rate of 98.41%. - Fouling can be mitigated by increasing the cross-flow velocity - The total operating cost of this system is about \$3.01/m^3, which is cheaper than the conventional treatment process. - The service life of the membrane was extended to more than 8 years.	[76]

(*continued on next page*)

Table 2 (*continued*)

Application and Examples				
Membrane	Pore size (nm)	Permeability (LMH/bar)	Remarks	Reference
Hollow fibre - ZrO_2	78	300 (wastewater)	- Oil rejection >99.7% - In particular, membrane fouling was effectively mitigated due to the critical role of electrostatic repulsion at a high pH value (>pH(IEP)). - Outstanding chemical stability and fouling resistance - Compared with conventional and commercial ceramic membranes, the developed ZrO2 membrane could reject nano-sized oil droplets (~18 nm) with over 99% rejection.	[69]
Tubular - ZrO_2 on Al_2O_3 support	<200	300 (wastewater)	- Oil rejection: 99.2% - Commercial Al_2O_3 MF membranes were modified by the nano-sized ZrO_2 coating, which reduced the membrane fouling and made the membrane more hydrophilic.	[70]
Hollow fibre MF - 8YSZ	580	1089 (clean water) 660 (emulsion)	- Oil rejection: 99.5% - Application of porous ceramic hollow fibre membranes in treating oily wastewater.	[72]
Tubular UF multichannel – ZrO_2 on SiC support	60	360 (clean water) 300 (wastewater)	- Oil rejection: 99.9% - Corrosion-resistant membrane (tested with 10% H_2SO_4 and NaOH at 60 °C) - No fouling observed	[73]
Drinking/Surface waters [11,54–59]				
Tubular MF - ZrO_2 on Al_2O_3 support	100	789 (lake water)	- Direct filtration of a lake water comparing four ceramic membranes (Al_2O_3, ZrO_2, TiO_2, SiC) and a PES/PVP polymeric MF membrane. - Commercial membranes by Atech innovations GmbH (Gladbeck, Germany). - Ceramic membranes presented much lower irreversible fouling than the polymeric one.	[11]
Hollow fibre (microtube) – YSZ with immobilized enzyme	200	–	- Bacteria filtration by immobilizing lysozyme as an antibacterial enzyme. - *Micrococcus luteus* bacteria retention of 99.9%.	[55]
Flat-sheet UF–ZrO_2/TiO_2 on ZrO_2/SiC support	6	160 (HA solution)	- One of the few ZrO_2 membranes on SiC support, which presented great retention of proteins (bovine serum albumin, whey protein, and hemoglobin), indigo dye, and humic acid. - Photocatalytic membranes effective in photodegrading phenol and humic acid under simulated sunlight irradiation. - Presented anti-fouling properties (smaller flux decline) and higher permeate flux under irradiation compared to the filtration in the dark.	[56]
Tubular MF - ZrO_2/TiO_2 on TiO_2 support	100	200 (AOM in water)	- Study of soluble algal organic matter (AOM) on fouling. - Commercial membrane CeRAM™ INSIDE, TAMI Industries. - A loose MF pre-filter (5 mm) or chemical coagulation may mitigate membrane fouling.	[57]
Tubular MF and UF–TiO_2/ZrO_2	200, 100, 300 KDa, 15 KDa	61, 60, 47, 37 (well water)	- Ground natural waters from a well containing E. coli bacteria were tested. - Ultrafiltration polymeric flat and ceramic MF and UF (tubular-multichannel) were tested to remove impurities from ground waters. - All membranes were efficient in disinfection by removing 100% of E. coli	[58]
Capillary UF- 3YSZ	55	30	- Virus filtration. - Increased pore sizes led to higher permeate fluxes but reduce virus retention. - A long-term virus filtration test for two weeks showed that membrane regeneration can be successfully applied by backflushing, which maintains a high permeate flux and permeate quality inside levels required by WHO and USEPA.	[59]
Organic Solvent filtration [51–53]				
Tubular – Hydrophobic modified ZrO_2 on Al_2O_3 support	200	1200 (Kerosene)	- The hydrophobic modification (hexadecyltrimethoxysilane) increases water rejection and reduces membrane fouling. - The water contact angle increased from 17° for the original membrane to 134° for the surface-modified membrane.	[51]
Tubular NF–Al_2O_3/ZrO_2 on Al_2O_3 support	1.4	10.3 (Ethanol) 1.3 (Toluene)	- Permeation experiments were operated with polar (ethanol) and non-polar (hexane, heptane, toluene) organic solvents. - Ceramic membranes do not demonstrate swelling as the polymeric ones.	[52]
	1.0	4.9 (Ethanol) 0.2 (Toluene)	- Polar solvents exhibited higher permeate flux own to the ceramic materials surface properties.	
Tubular NF–ZrO_2/TiO_2 on Al_2O_3 support	1.0	2.8 (Methanol) 0.82 (Ethanol) 0.45(nOctane)	- The permeation mechanism was affected by membrane-solvent interaction, solvent viscosity, and molecules occupied area. - Dye rejections in methanol: “evans blue” (>90%), acid red 265 (>90%), methyl orange (>90%).	[53]
Pre-treatment for RO [61]				
Flat-sheet UF–ZrO_2/SiO_2 on Al_2O_3 support	50	1654 (water) 51 (wastewater)	- Treatment of a semiconductor wastewater. - Ceramic membrane was combined with ozone to reduce TOC and turbidity before the RO with polymeric membranes. - The pre-treatment reduces energy consumption in the RO step.	[61]
Gas separation/Pervaporation [66,67]				
Tubular – ZrO_2 on Al_2O_3 support	<1	–	- Membranes were selective in pervaporation dehydration of a water/n-butanol mixture. - ZrO_2 membrane showed stable separation performance for 120 days with a high selectivity towards water.	[66]
Food industry & Protein filtration [77–86]				
Tubular MF – ZrO_2	200	9.5 (soya sauce)	- Raw soya sauce filtration - Comparison between ZrO_2 (0.2 μm) and Al_2O_3 (0.2, 0.5, 0.8 μm) membranes. 0.2 μm Al_2O_3 membrane had the best permeate quality and flux. - More than 99% of bacteria could be removed from raw soy sauce.	[82]

(*continued on next page*)

Table 2 (*continued*)

Application and Examples				
Membrane	Pore size (nm)	Permeability (LMH/bar)	Remarks	Reference
			- The fouling resistance of the ZrO_2 membrane was dominated by concentration polarization resistance, the membrane's own resistance), cake resistance and internal fouling resistance remained negligible.	
Tubular - ZrO_2 grafted with polymer	200	66 (BSA)	- Grafted membrane exhibited good anti-fouling properties and higher removal of BSA (84.9%). - Using the alternate temperature-change cleaning process, a water flux recovery of about 80% was obtained.	[83]
Tubular UF–ZrO_2 on Al_2O_3 support	7	135 (water) 80 (BSA)	– 100% retention of BSA. - The prepared membrane showed excellent corrosion resistance and antifouling properties.	[84]
Tubular UF–ZrO_2 on Al_2O_3 support	100	400 (10 °C) 1000 (55 °C)	- Milk protein fractionation - Comparison between TiO_2, Al_2O_3, and ZrO_2 membranes with 100 nm pore size. - ZrO_2 presented the higher flux and better fouling behaviour.	[86]
Tubular UF–ZrO_2 on Al_2O_3 support	50	280 (water) 40 (protein)	- Cross-flow filtration of whey protein solutions comparing ZrO_2 (50 nm) and Al_2O_3 (200 nm) membranes. Commercial Membralox membranes (SCT, Bazet, France) were used. - The protein adsorption resistance controls the flux to a greater extent for the alumina membrane than for that with zirconia, where a resistance due to fouling tends to dominate.	[77]
Radioactive waste filtration [60]				
Tubular NF–ZrO_2/Al_2O_3 on Al_2O_3 support	1 KDa	14 (clean water)	- The highest uranium rejection was 91% at pH 7.4, in which the negatively charged uranium species had an electrostatic attraction to the positively charged membranes. - Uranium species in a natural aquatic system could be effectively removed by the fabricated ceramic NF membranes	[60]

LMH/bar: L m^{-2} h^{-1} bar^{-1}, YSZ: yttria-stabilised zirconia, BSA: bovine serum albumin, HA: humic acid, AOM: dissolved extracellular algal organic matter.

Table 3
Commercial ZrO_2 and ZrO_2/TiO_2 ceramic membranes for ultrafiltration and nanofiltration. Elaborated with data supplied by the manufactures [89–95] and found in the literature [13,17,30,71,73,77,96,97]. Some data were not disclosed by their manufactures nor found in the literature.

Company	Product	Support	Top layer	Type	Pore size and/or MWCO	Water permeability (LMH/bar)	Reference
Pall Corporation	Membralox®	α- Al_2O_3	ZrO_2	UF	20 nm 50 nm 100 nm	400 800 1500	[77,95]
TAMI industries	INSIDE CéRAM™	α- Al_2O_3	ZrO_2	UF	5–30 nm	<40	[22,94,98]
Inopor	inopor® ultra	α- Al_2O_3	ZrO_2	NF UF	3 nm (2 kDa) 110 nm	N.A.	[93]
Groupe Novasep	Kerasep®	TiO_2/Al_2O_3	ZrO_2/TiO_2	UF Fine UF	15–300 kDa 1–3 kDa	96 (15 KDa) N.A.	[92,99]
Tech-Sep	Carbosep	C	ZrO_2	UF	10 KDa 15 KDa	57 88	[81,99]
CTI-ORELIS, ALSYS group	Kleansep™	TiO_2/Al_2O_3	ZrO_2/TiO_2	UF NF	8–300 kDa 1–5 kDa	N.A.	[91]
Atech Innovations	–	α-Al_2O_3	ZrO_2; TiO_2	UF NF	100 nm 10–150 kDa 1–5 kDa	700 N.A.	[86,90]
Gaston County Filtration systems	Ucarsep®	–	ZrO_2	UF	4–20 nm	45–250	[71,89]

N.A.: not available; LMH/bar: L m^{-2} h^{-1} bar^{-1}.

characterisation and application. Table 4 presents a compilation of remarkable works published concerning the fabrication of UF and NF zirconia membranes.

In a pioneer work, Larbot et al. [104] applied a colloidal sol-gel route to prepare crack-free microporous alumina, titania, and zirconia membranes on α-Al_2O_3 microfiltration supports. As a result, these authors obtained UF ZrO_2 membranes with pore sizes from 6 to 10 nm and water permeability values between 175 and 210 L m^{-2} h^{-1} bar^{-1}, respectively. In addition, no detectable corrosion after tests in pH values of 0.5 and 13.5 at 80 °C for 24 h.

A few years later, Etienne et al. [107] fabricated a tubular zirconia NF membrane with an average pore size of around 4 nm, achieving up to 90% retention of dextran (10 kDa). Later, with an intent to avoid excessive sol infiltration on YSZ substrates, Okubo et al. [112] combined a polymeric sol with a colloidal sol, producing a crack-free YSZ membrane. The sol was composed of zirconium tetra-n-butoxide and triethanolamine as a chelating agent. Unfortunately, no pore size distribution or water permeability were provided.

Later, Vacassy et al. [113] developed a microporous MgO–ZrO_2 membrane in which the ZrO_2 cubic phase, obtained by adding 13 % molar of MgO, was stable up to 1170 K. The produced membranes presented saccharose (MW = 542 g mol^{-1}) and vitamin B12 (MW = 1355 g mol^{-1}) retentions of 54 and 73%, respectively. Benfer et al. [110] obtained a NF zirconia membranes with pore size around 1–2 nm and a relatively high water permeability (80 L m^{-2} h^{-1} bar^{-1}) since the support was also composed of ZrO_2, which is more hydrophilic than alumina, leading to higher water fluxes. These authors observed a SO_4^{2} rejection of 66.3%.

Van Gestel et al. [34] fabricated disk ZrO_2 membranes for NF with a MWCO lower than 300 Da in alumina supports. Long-term corrosion tests demonstrated that the fabricated membranes were corrosion resistant under pH values of 13 and 1. Kreiter et al. [66] applied microemulsion-based acetylacetonate-stabilised zirconia sol to prepare a membrane that was selective in pervaporation dehydration of a

Table 4
Outstanding works in the fabrication of ultrafiltration (UF), nanofiltration (NF), and pervaporation (PV) zirconia membranes.

Type	Material (Phase)	Support (Pore size)	Sol gel route	Sintering Temperature (°C)	Top layer thickness (nm)	Water permeability ($Lm^{-2}h^{-1}bar^{-1}$)	MWCO (Da)	Pore size (nm)	Test	Reference
UF	ZrO_2 (M, T)	SiC (5 μm)	C	700	$63_x 10^3$	355	$2x10^6$	65	–	[106]
	ZrO_2 (M)	SiC (2–10 μm)	–	1125	$45_x 10^3$	360	–	60	Oil/Water, Corrosion, Laundry Wastewater	[46,73]
	ZrO_2 (M, T)	α- Al_2O_3 (200 nm)	C	470–1170	6–10	175–210	–	6,8,10	Corrosion	[104]
	ZrO_2 (T)	γ- Al_2O_3 (5 nm)	C	450	150	2–3	–	4	Dextran	[107]
NF	ZrO_2 (T)	γ- Al_2O_3 (5–6 nm)	P	400	100	0.20	1200	1–2	PEG, Salts, Corrosion	[108]
	ZrO_2 (T)	α- Al_2O_3 (75 nm)	C	500	200	22.5	1150	1.6	PEG, BSA, Dyes, WW	[109]
	ZrO_2 (T)	ZrO_2 (60 nm) + ZrO_2 (5 nm)	P	500	50	80	1000	1–2	Dyes, Salts	[110]
	Y–ZrO_2 (T)	ZrO_2 (5.5 nm)	C	400	100	25	840	1.4	PEG, Dextran, Salts	[111]
	Y–ZrO_2 (T)	α-Al_2O_3 (1000 nm) + γ-Al_2O_3 (75 nm) + γ-Al_2O_3 (5 nm)	P	500	260	3.9–4.2	800	1.4	PEG, Pesticide	[41]
	Y– ZrO_2 (T)	ZrO_2 (18 kDa)	C	400	100	28	800		Dye, NaCl	[47]
	ZrO_2 (T)	Al_2O_3 (10 nm)	C	400	180	13	750	1.3	PEG, NaCl	[31]
	ZrO_2	γ- Al_2O_3 (5–6 nm)	P	350–400	–	0.2–0.3	354–1195	0.9–1.7	Salts, PEG	[16]
	Y–ZrO_2 (T)	α-Al_2O_3 (80 nm) + ZrO_2 (3.6 nm)	C,P	400	50	2.28	200–300	0.7–0.8	PEG, Corrosion	[34]
PV	ZrO_2 (T)	γ- Al_2O_3 (4 nm)	P	300–380	110	–	–	<1	Gas, PV	[66]

PV: pervaporation, C: colloidal sol-gel, P: polymeric sol-gel, T: tetragonal ZrO_2, M: monoclinic ZrO_2, WW: wastewater.

water/n-butanol mixture, with a stable separation performance for 120 days. Further, Zhu et al. [108] investigated the effect of sol size on the NF performance of zirconia membranes, showing that the sol size is one of the key factors in obtaining a continuous and defect-free membrane. These authors stated that the average size of the sol should be below 12 nm since the zirconia sol will retain a low branched polymeric nature and allow interpenetration of polymer chains.

Recently, Da et al. [111] demonstrated the importance of the intermediate layer on the properties of the final membranes. These authors prepared a crack-free YSZ NF membrane layer with an MWCO of 816 Da, a retention rate towards $MgCl_2$ of 71%, and a relatively high water permeability of 25 L m^{-2} h^{-1} bar^{-1}. As shown in Fig. 3, the highest water permeability values reported for the NF zirconia membranes were obtained when ZrO_2 substrates/intermediate layers were used [47,110,111] since ZrO_2 is more hydrophilic than alumina, reducing water permeation resistance [70,106,114].

Concerning characterisation and testing microporous ZrO_2 membrane, most papers report measurement of clean water permeability and PEG (or dextran) retention to calculate MWCO and estimate the pore size [16,34,66,111]. In some cases, for pores below 1 nm, gas permeation was applied to estimate pore dimension [66,115]. Regarding corrosion, good studies can be found in Refs. [24,34,88,104,108]. For ZrO_2 NF membranes, own to their high zeta-potential, salt separation was usually evaluated [16,31,47,108,111]. For instance, Guo et al. [116] obtained >80% of $MgCl_2$ and $CaCl_2$ using a developed ZrO_2–TiO_2 NF membrane with MWCO 620 Da and water permeability 0.12 L m^{-2} h^{-1} bar^{-1}.

With an increasing interest in new wastewater treatments, ZrO_2 membranes stand out as a potential candidate for treating heavily polluted [37] or oily feeds [71,117] own to zirconia's extraordinary chemical stability and high hydrophilicity [73]. Some authors investigated the removal of dies from synthetic [109,110] and real wastewaters [46,47]. Bernfer et al. [110] obtained 99.2% retention of the dye "Direct red" (MW = 991 g mol^{-1}) and a permeate flux of 26 L m^{-2} h^{-1} with a ZrO_2 NF membrane operating at 2 bar. However, for a smaller dye such as "Orange G" (MW = 452 g mol^{-1}), the retention dropped to only 30%,

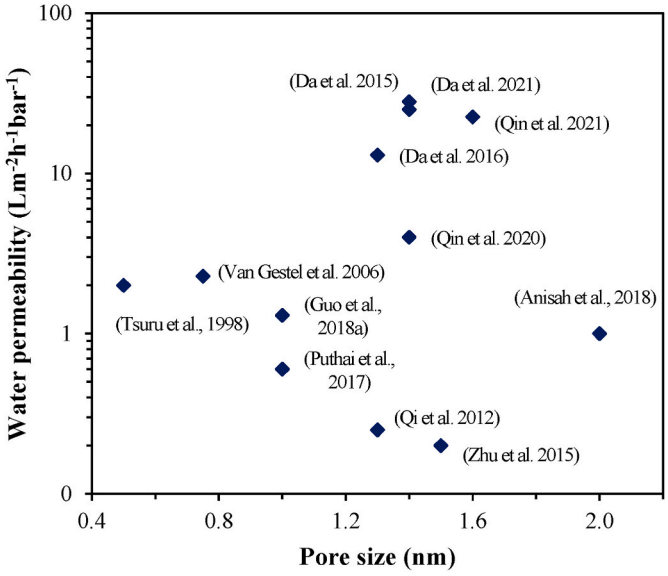

Fig. 3. Pure water permeability versus average pore size for zirconia-based membranes reported in the literature.

which indicated the MWCO of the fabricated membranes was close to 1000 Da. Working with a wastewater originating from the dyeing process, Da et al. [72] recovered 99% of a fluorescent brightener (MW = 1100 g mol^{-1}) at a permeate flux of 89 L m^{-2} h^{-1} at 10 bar and 60 °C. These authors developed an NF YSZ membrane with MWCO of 800 Da on a homemade UF ZrO_2 support. Luogo et al. [46] compared a MF SiC membrane and a UF ZrO_2 membrane for the treatment of a laundry wastewater. As a result, the zirconia membrane presented less fouling and a higher removal of microplastics (99.2%) compared to the silicon carbide membrane (98.5%).

Qin et al. [109] tested their ZrO_2 NF membrane (1150 Da) in the

filtration of several water-soluble dyes with different molecular weights. As a result, retentions of methyl red (MW = 270 g mol^{-1}) and methyl orange (MW = 327 g mol^{-1}) were both <65% due to their small molecular size. On the other hand, for the dyes alizarin red (MW = 360 g mol^{-1}), direct red (MW = 660 g mol^{-1}), bromocresol green (MW = 698 g mol^{-1}), and methyl blue (MW = 800 g mol^{-1}) retention values of 98.5%, 99.2%, 99.5%, and 99.6%, respectively, were obtained. This result could not be explained by size exclusion since these dyes are smaller than the membrane MWCO. Therefore, the authors stated that the dye molecules' aggregation enlarges their effective size, enhancing the dye rejection and forming a secondary polarization layer in the form of a gel on the membrane surface. As a result, after a long-term operation, the membrane fouling becomes severe, requiring cleaning to restore the initial permeate flux. Neither backwashing nor acid/alkaline washing were not effective in removing the dye molecules absorbed on the membrane surface, which required the calcination of the membrane at 300 °C.

As an alternative to chemical cleaning or calcination, the biofouling and fouling caused by organic compounds could be avoided by functionalising the membrane surface with nanomaterials (*e.g.*, antimicrobial nano-Ag, CNTs (carbon nanotubes), and catalytic MnO_2 and Fe_2O_3) [17], or with photocatalytic materials (*e.g.*, TiO_2 [118–122] and ZrO_2 [42,56]). Catalytic coatings or active layers can provide anti-fouling and self-cleaning properties to the membrane, as the one prepared by Bortot Coelho et al. [56], who developed a Ce–Y–ZrO_2/TiO_2 UF photocatalytic membrane with a pore size of 6 nm on ZrO_2/SiC supports. The photocatalytic top layer was able to degrade phenol and humic acid under simulated solar light irradiation while presenting better anti-fouling properties: a smaller flux decline and higher permeate flux under irradiation compared to the filtration in the dark. Moreover, self-cleaning properties were observed by irradiating the membrane, which recovered up to 97% of the original flux. Consequently, a longer operation without chemical cleaning would be possible, reducing costs and the process footprint (Fig. 4).

The same membrane was evaluated for the treatment of an effluent from an urban wastewater treatment plant by Deemter et al. [42]. These authors reported that original permeate flux conditions could be fully recovered after exposing the membrane to solar light irradiation. In addition, the photocatalytic membrane significantly reduced the turbidity of the effluent, significantly increasing the degradation efficiency of the subsequent solar photo-Fenton treatment. The results showed that the membrane allowed consistent retention of *Pseudomonas Aeruginosa* at an order of magnitude of 10^3–10^4 CFU mL^{-1}, which demonstrated the membrane's enhanced water disinfection capability and pointed to the development of innovative treatments for dinking and wastewaters by combining filtration and advanced oxidation processes for abatement of contaminants of emerging concern in the presence of natural organic matter. Nevertheless, some aspects need to be considered before implementing this technology, such as the design of the photocatalytic membrane reactor that should allow light irradiation of the membrane and be resistant to elevated cross-flow conditions and high pressures [17]. Other factors, such as the intermediate products of organic pollutants in the catalytic process, the extension of hydraulic retention time in the reactor, the energy consumption, and the environmental impacts of the novel system should be further investigated/optimized before the industrial implementation of this technology.

3. Fabrication of ZrO_2 membranes by sol-gel techniques

The first step in the fabrication of UF and NF zirconia membranes is selecting the support, which can be made of zirconia or other ceramic materials, such as α-alumina [123] and silicon carbide [106]. The support usually has pore sizes around 2–10 μm and is responsible for the membrane's mechanical strength, and its selection is usually based on the mechanical strength requirement and factors such as chemical resistance and durability [124] since most pressure drop occurs in the separation layer [10,125]. Nevertheless, to obtain a defect-free homogenous separation layer, the support pore size and surface roughness should be strictly controlled; it is recommended a roughness lower than 1 μm [126]. The support fabrication is not discussed in this review.

For supports with pore sizes larger than the micro- or ultrafiltration range, it is necessary to add intermediates layers before reaching the final nanofiltration layer. There are several processes to incorporate intermediate/top layers on the support, such as coating with a particle suspension (slurry), sol-gel formation, physical vapour deposition (PVD), chemical vapour deposition (CVD), molecular layer deposition (MLD), and electrolytic deposition [10,13]. Since the sol-gel coating is the most applied method for fabricating ultra- and nanofiltration zirconia membranes, the most critical parameters in the synthesis and the relations between syntheses, microstructure, and membrane properties are reviewed next.

Sol-gel processes were introduced in the 1980s to prepare mainly MF and UF membranes and, later on, NF membranes [127]. Although 330 documents were published addressing the sol-gel fabrication of zirconia membranes from 1980 to 2021, based on the Scopus database [128], most of the literature available focus on alumina and silica membranes. Currently, there is still no literature review focusing on the fabrication of ZrO_2 membranes.

Generally, a sol-gel process consists of the preparation of the gel, its deposition on the support, a drying step, and finally, the sintering. For the preparation of the gel, the processing conditions (*e.g.,* precursor, solvent, pH, and catalyst) lead the reaction towards the formation of either colloidal or polymeric gels (Fig. 5).

– Colloidal gels are usually prepared in aqueous media, in which steric and electric effects between colloids in the sol dominate gel formation [127]. This route leads to larger pores being applied in the preparation of meso- and microporous layers.

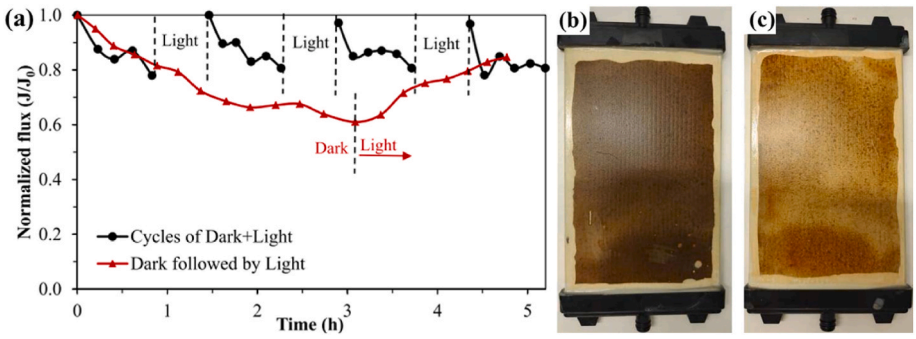

Fig. 4. (a) Normalised permeate flux for humic acid filtration experiments using a Ce–Y–ZrO_2/TiO_2 UF photocatalytic membrane under dark and light irradiation intervals; Pictures of the membrane after HA filtration (b) in the dark and (c) under irradiation. Source: adapted from Ref. [56].

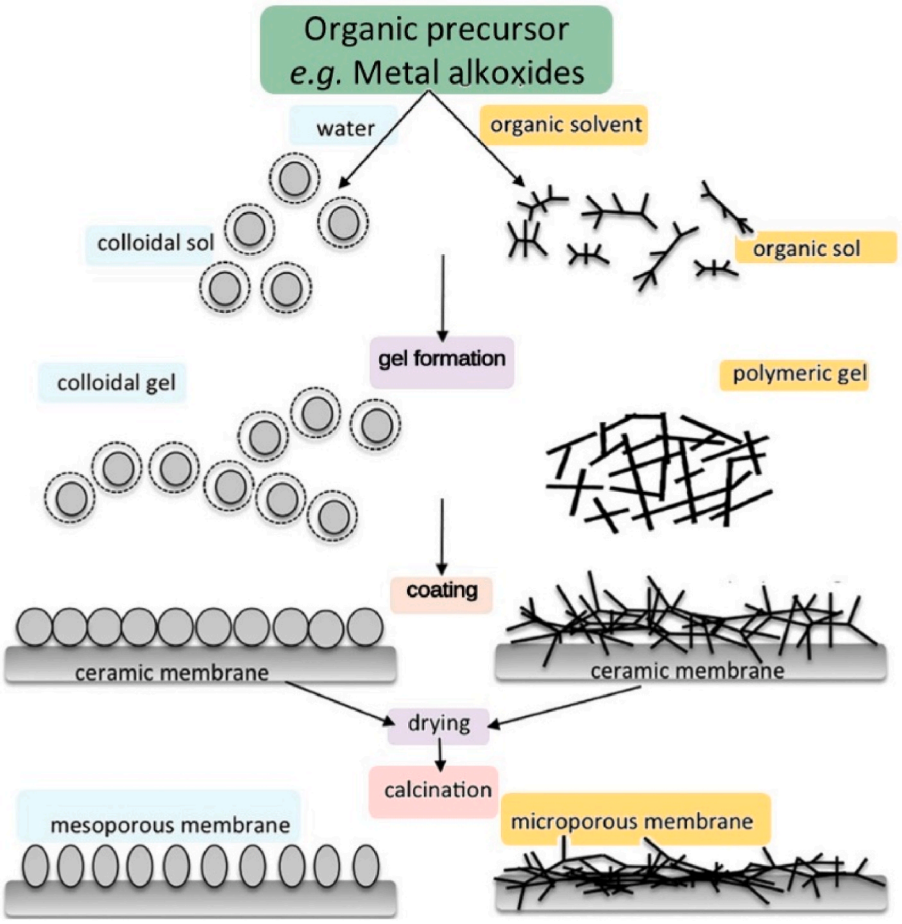

Fig. 5. Colloidal and polymeric sol-gel routes. Source: Adapted from Ref. [13].

– Polymeric gels are mostly obtained in organic media, in which the relative rates and extents of hydrolysis and condensation reactions promote polymerisation and branching, formatting a crosslinked gel [129]. This route leads to microporous or almost dense top layers [127].

Once formed, the gel can be applied to the support using dip coating [34,130], slip casting, and spin coating [131]. Briefly, in the dip-coating method (Fig. 6a

), the support is soaked into the gel solution. By capillary forces, the solvent is sucked into the support, which is then removed at controlled speeds, and the support gets coated with the gel film. In the spin coating

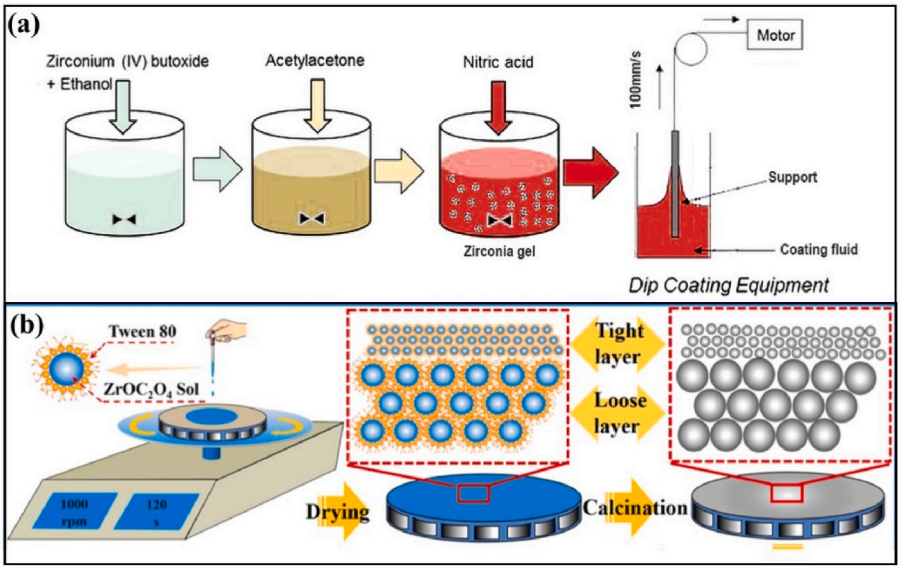

Fig. 6. (a) Dip coating process and (b) spin coating process. Source: adapted from Ref. [109].

method, the coating fluid is applied at the centre of the rotating substrate by centrifugal force, and the coating spins off the support until the desired film thickness is achieved (Fig. 6b).

After the gel drying, the solvents and part of the by-products are removed, and the xerogel is obtained. Finally, a sintering/calcination is performed to obtain the ceramic membrane. The main advantage of a sol-gel process is getting tiny pores with specific shapes and size distribution. Nevertheless, several factors, such as the precursor, the hydrolysis ratio, alcohol/Zr ratio, acid/Zr ratio, peptization conditions, phase stabilisers, additives, and the sintering temperature, need to be considered to tailor the properties of the membrane and to avoid defects in the top layer. Each of these parameters is discussed in the following paragraphs.

3.1. Precursors and solvents

The precursors generally utilised in sol-gel processes for ZrO_2 separation layers are zirconium alkoxides (*e.g.,* $Zr(OC_3H_7)_4$) and zirconium salts (*e.g.,* $ZrOCl_2$, $Zr(NO_3)_4$). Both have their advantages and different uses. While the organic precursors are suitable for colloidal and polymeric routes, they are usually toxic, flammable, and unstable reagents [132]. On the other hand, salt precursors are cheaper and greener [31,116], but they produce only colloidal gels since they need to be dissolved in water [127]. During the gel formation from the alkoxides, the reactions occurring are hydrolysis (Eq.(1)) and condensation (Eq.(2)). In hydrolysis, water reacts with the alkoxide and removes or replaces –R for H. In condensation reactions, the Zr(OR)n or hydrolysed alkoxide reacts with each other to form chains, releasing water or alcohol [133,134].

$$Zr(OR)_n + H_2O \rightarrow Zr(OR)_{n-1}(OH) + ROH \quad (1)$$

$$Zr(OR)_n + Zr(OR)_{n-1}(OH) \rightarrow Zr_2(OR)_{2n-2} + ROH \quad (2)$$

Zirconium propoxide ($Zr(OC_3H_7)_4$), usually found in propanol solutions, is the most frequent precursor reported in the literature [34,41,108,110], followed by zirconium butoxide ($Zr(OC_4H_9)_4$) [131,135]. Rossignol [136] compared zirconium butoxide and propoxide, but no significant differences were observed in terms of particle size and surface area. Zirconium alkoxides are considerably more reactive than other alkoxides, following the order $Si(OR)_4 \ll Sn(OR)_4 = Ti(OR)_4 < Zr(OR)_4 = Ce(OR)_4$ [137]. Therefore, the first difficulty in synthesising zirconia sols is controlling the fast hydrolysis of its alkoxides [138]. For the formation of polymeric gels, the alkoxides are usually diluted in an anhydrous organic solvent to prevent fast hydrolysis and the formation of big particles [50]. The concentration of the organic precursor is also essential, and as a general rule, it needs to be kept as low as possible, in the range of 0.01–0.5 mol L^{-1} [16,106] in alcohols, such as isopropanol [135], ethanol [130], and butanol [131]. Another possibility is to use chelating agents as stabilisers, which are discussed in detail in the following items.

The zirconium salts precursors typically applied for the preparation of colloidal gels are $ZrOCl_2$ [31,106] and $Zr(NO_3)_4$ [37]. $ZrCl_4$ is also a well-known zirconia precursor, but since it rapidly hydrolysis in the presence of humidity [70], it requires working under dry conditions, such as in a controlled atmosphere glove box. In the same way as for the polymeric sol-gel, in the colloidal route, the zirconium concentration should be kept low to control the particulate size since it will affect the microstructure of the membrane layer after drying and heat treatment [133]. Typically found concentrations are in the range of 0.01–0.1 mol L^{-1} [31,37,106]. Coterillo et al. [139] reported that higher concentrations of zirconium tetra-n-butoxide in colloidal gels, prepared in a water/ethanol mixture with HCl as a catalyst, led to bigger particle sizes in the sols and larger pore sizes after sintering (Table 5). Da et al. [47] obtained similar results with colloidal sols prepared at a refluxing temperature of 80 °C and a $[H_2C_2O_4]$:$[ZrOCl_2]$ molar ratio of 0.2:1, as shown in Fig. 7a. The precursor concentration affects not only the sol size but also the properties of the calcined membrane, as reported by Da et al. [111], which fabricated 8YSZ (Yttria Stabilised Zirconia, 8% molar yttria) top layers on ZrO_2 UF membranes with a pore size of 5.5 nm. In Fig. 7b, it can be seen that a drastic decrease in PEG retention was observed with a sol concentration of 0.1 mol L^{-1} due to the top layer cracks propagation. Depending on the pore size of the support, the gel size needs to be big enough to avoid the excessive infiltration of the coating into the support but small enough to keep the final membrane pore size as low as possible, as reported by Zhu et al. [108] in the fabrication of microporous ZrO_2 membranes on alumina substrates.

Table 5
Effect of the precursor concentration on particle size and resulting pore size of colloidal sols. Source: adapted from Ref. [139].

Zirconium butoxide		Mean particle size	Mean pore size
[wt. %]	[mol L^{-1}]	[nm]	[nm]
2.0	0.052	27.5	6.5
1.5	0.039	21.8	4.1
1.0	0.026	14.0	3.5
0.7	0.018	12.6	<3.0
0.5	0.013	7.8	–

3.2. Dopants

Pristine ZrO_2 presents three polymorphs: monoclinic $\overset{\Delta}{\rightarrow}$ tetragonal $\overset{\Delta}{\rightarrow}$ cubic, which can be transformed one in the other by heating, as indicated in Fig. 8a. The symmetric cubic ZrO_2 phase forms at temperatures above 2370 °C [13,35], while the transformation between the tetragonal to the monoclinic form occurs around 1173 °C, which is accompanied by a large volume variation (~4–9%) that can cause cracks in the membrane layer.

In sol-gel syntheses, the main phase formed after the sintering of pristine zirconia is the metastable tetragonal ZrO_2, which can also be accompanied by the monoclinic phase [47,107,108,110]. However, when this pristine ZrO_2 is submitted to high temperatures (starting from 450 to 700 °C or higher) during sintering or operation, the phase transformation from tetragonal to monoclinic is observed [140], as shown by the diffractograms in Fig. 8b. This transformation causes an increase in the pore size, and it can cause cracks formation in the deposited layer [31]. Several techniques have been proposed to stabilise the tetragonal or cubic polymorphs (Fig. 8c) by doping ZrO_2 with yttria (3–10 %mol Y_2O_3), calcium oxide (12–13 mol% CaO), magnesium oxide (MgO), or rare-earth oxides (8–12 mol%), such as Yb_2O_3, Nd_2O_3, and Sm_2O_3 [141]. The addition of doping elements, such as the cations magnesium [113], cerium [142], and aluminium [143], creates oxygen ion vacancies in the zirconia lattice to form energetically favoured structures [31,144] or promotes the internal compression within the zirconia lattice, increasing strain energy and release of deformation energy, therefore inhibiting the phase transformation [37]. In addition, the mixture of ZrO_2 and TiO_2 can stabilise tetragonal ZrO_2 [37], which will be discussed in detail in a further section.

Yttria-stabilised zirconia (YSZ) is the most studied material own to its high strength and fracture toughness [150], combined with high corrosion and temperature resistances, which make this material suitable for high-performance ceramics, such as solid oxide fuel cell electrodes and medical implants [151]. Fig. 8d shows a phase diagram of the ZrO_2/Y_2O_3 system, proposed originally by Scott [147], in which can be inferred that depending on the amount of yttria added and the temperature, either tetragonal or cubic phases can be stabilised [149]. Nevertheless, as reported by Yashima et al. [148], metastable phases can be formed depending on the sintering conditions. The two compositions usually reported [152,153] are the partially stabilised 3YSZ (3 mol% Y_2O_3 or 5.8 mol% $YO_{1.5}$) and the fully stabilised 8YSZ (8 mol% Y_2O_3 or 14.8 mol% $YO_{1.5}$). Membranes developed with 8YSZ have demonstrated increased thermal stability, even at 700 °C or under hydrothermal

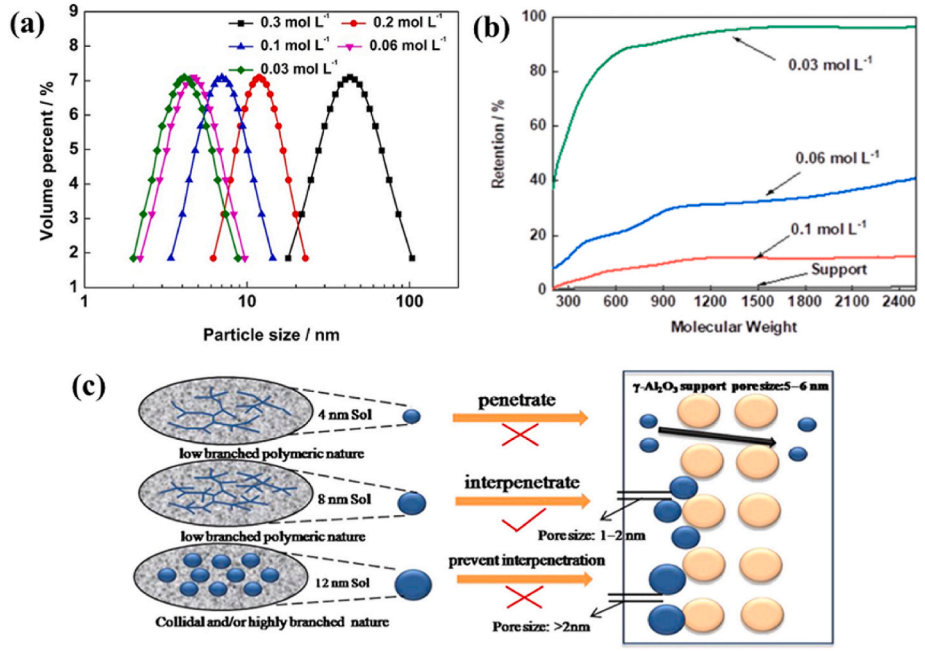

Fig. 7. (a) Effect of Zr precursor concentration on: (a) gel size (Source: adapted from Ref. [47]) and (b) PEG retention (Source: adapted from [111]); (c) Effect of sol size on the coting infiltration into the support (Source: adapted from Ref. [108]).

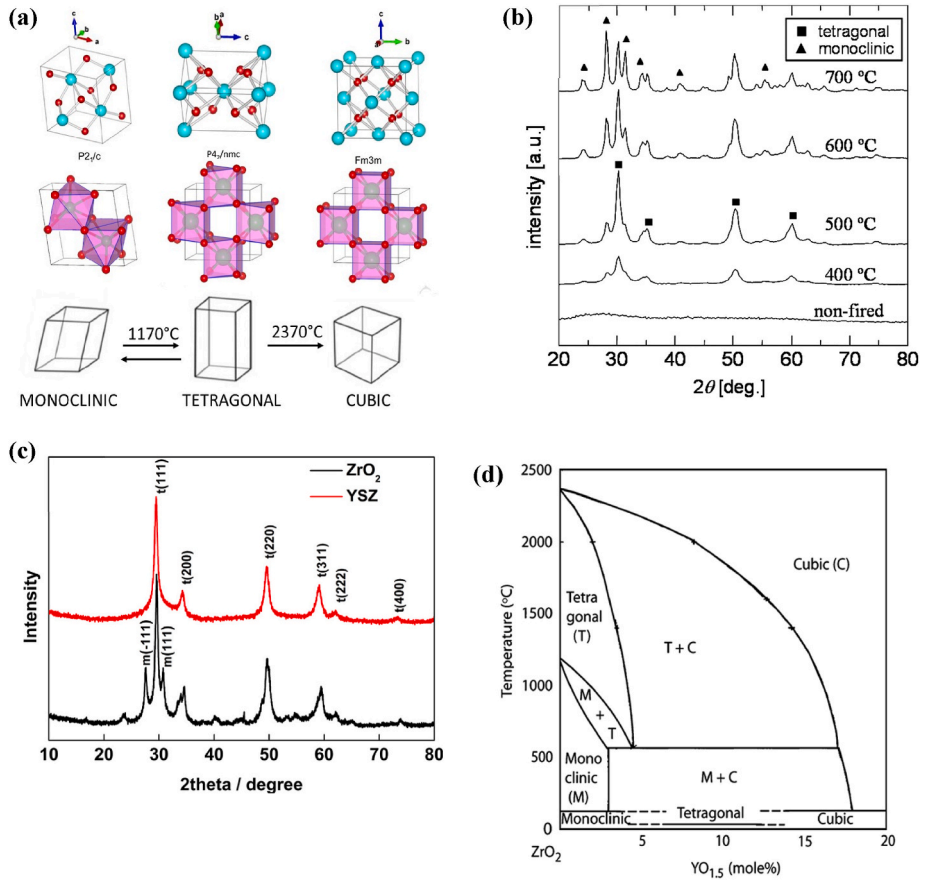

Fig. 8. (a) Polymorphs of ZrO2. Source: Elaborated based on [145,146]; (b) X-ray diffractograms of pristine ZrO2 membranes sintered at different temperatures. Source: [139]; (c) X-ray diffractograms of pristine ZrO2 and yttria-stabilised zirconia fired at 400 °C. Source: [47]; (d) ZrO_2/Y_2O_3 phase diagram. Source: [147–149].

conditions [19,88].

Regarding the fabrication of YSZ membranes, following the colloidal sol-gel route, Da et al. [47] added $Y(NO_3)_3.6H_2O$ after forming the sol with $ZrOC_2O_4$ to obtain a Y:Zr ratio of 8:92. As a result, only the tetragonal phase was obtained after calcination at 400 °C, and the sol size was slightly smaller (4.1 nm) than the ones obtained for pristine zirconia (4.7 nm). Yttrium nitrate was also the salt used by Van Gestel et al. [34] to prepare a 3YSZ sol from zirconium propoxide. As a result, the membranes calcined at 450 °C presented only a tetragonal phase and were crack-free. Concerning the polymeric sol-gel route, tetragonal 8YSZ membranes were prepared with yttrium isopropoxide ($Y(OC_3H_7)_3$) [88] and with yttrium nitrate ($Y(NO_3)_3{\cdot}6H_2O$) [41], both added to zirconium propoxide. As a result, the Y-doping avoided membrane cracks during sintering, as shown by the SEM images of the surface of the membrane made of pristine ZrO2 (Fig. 9a) and 8YZS (Fig. 9b).

3.3. Polymeric sol-gel: Hydrolysis ratio and stabilisers

In the polymeric sol-gel route, an oxide network is formed by controlling the hydrolysis and polymerisation (condensation) reaction rates. However, the kinetics of formation for zirconia and titania sols are much faster than for silica-based sols [154] since the hydrolysis reactivity of the precursors increases in the order Si ≪ Ti\Zr [155]. The reason is that the alkoxides react with water depending on the metals' electronegativity and unsaturation number (steric effect): coordination number-oxidation number, which determines the partial charge on the metal atoms (δ): while Si alkoxides exhibits a $\delta = +0.32$, Ti and Zr possess higher partial charges, +0.63 and + 0.74, respectively [129]. In this respect, the fast hydrolysis of zirconia precursors requires careful control of the amount of water present, the temperature, and the concentrations of precursor and organic ligands. As discussed previously, the precursor concentration must be kept low to obtain sols with small particle sizes. The effects of the amount of water (hydrolysis ratio) and the addition of organic ligands (stabilisers) are discussed next.

The hydrolysis ratio (HR) is defined by the number of moles of water added in the sol-gel process divided by the number of moles of propoxide utilised. Higher HR values imply the complete hydrolysis of the precursor, which corresponds to the colloidal route and leads to bigger particle sizes. On the other hand, the polymeric route, producing sols with smaller particle sizes, occurs with the partial hydrolysis of the precursor, obtained with lower hydrolysis ratios. For example, Qi et al. [16] studied the particle size of polymeric ZrO_2 sols obtained from zirconium n-propoxide (ZrPR) as precursor and diethanolamine (DEA) as a chelating agent ([DEA]/[ZrPR] = 2.2). As shown in Fig. 10a, the average particle size of the sol increased from 5.7 nm with an HR of 5–8.9 nm with an HR of 9.4, owing to the accelerated hydrolysis reaction rate at a higher HR. This result is also valid for mixed oxides, Lawal et al. [115] prepared SiO_2–ZrO_2-acetylacetone gels in ethanol using zirconium (iv) tert-butoxide (ZrTB), tetraethoxysilane (TEOS), acetylacetone (acac/ZrTB molar ratio = 4/1) as a stabiliser, and hydrochloric acid as catalyst (acid/alkoxide molar ratio 0.25). Increasing HR from 4 to 240 led to an average sol size increasing from 3.4 nm to 12 nm (Fig. 10b), which was attributed to more condensation reactions between -SiOH and -ZrOH hydrolysed groups. As expected, the membranes fabricated with sols of higher HR values had larger pore sizes and less selective gas separation capacity [115].

Too small particle sizes can cause excessive sol infiltration into the support [34] or result in completely dense membrane structures, as reported by Van Gestel et al. [88]. These authors fabricated a ZrO_2 membrane, which was impermeable to water under a *trans*-membrane pressure of 10 bar (1 MPa), by using a sol with an average particle size of 6 nm.

Unfortunately, the control of the amount of water or the use of a low concentration of precursor may not be enough to avoid the fast hydrolysis of the precursor [31] and ensure the sol stability [16], as the presence of water in the solvent, support, and air play a not neglectable role. Therefore, the strategy is to reduce the precursor hydrolysis rate by adding chelating ligands such as acetic acid, acetylacetone (acac), and diethanolamine (DEA) [41,110,113,131,156]. Benfer et al. [110] compared these stabilisers and observed that acetylacetone completely stabilises the alkoxide-additive complex, while acetic acid is less effective than DEA. As shown in Fig. 10c, the viscosity of a zirconium propoxide sol increases gradually with the water addition, caused by the controlled polycondensation reaction. However, after adding 1.5 and 3.5 mol of water to a sol stabilised with acetic acid and DEA, respectively, a significant increase is observed due to the loss of stabilisation effect. Qi et al. [16] observed that by increasing the ratio between DEA and zirconium propoxide, the average particle size of the sols was reduced while the size distribution became narrower, as shown in Fig. 10d.

Another approach to control the rapid hydrolysis of Zr-alkoxides to keep a small sol particle size, proposed by Shah et al. [138], is to avoid the direct addition of water to promote the alkoxide hydrolysation, but to exploit the water released from the reaction between acid and alcohol or from the condensation/oxolation reaction. Applying this technique, these authors obtained pores small enough to promote H_2/CO_2 separation when coating an alpha-alumina support.

In summary, the particle size of the sol needs to be controlled as the sol size directly affects the infiltration of the gel into the support and the final membrane permeability [16]. This can be achieved by setting several parameters, such as precursor concentration, hydrolysis ratio, kind of stabilisers, dopants, hydrolysis time and temperature.

3.4. Colloidal sol-gel: Additives

Controlling the size of colloidal sols is challenging due to the rapid hydrolysis and condensation of precursors when an excess of water is used [37,157]. Moreover, obtaining stable colloidal sols with particle sizes smaller than 10 nm is not trivial due to particles' aggregation and packing [158,159]. To avoid these issues, some additives (*e.g.,* chelating

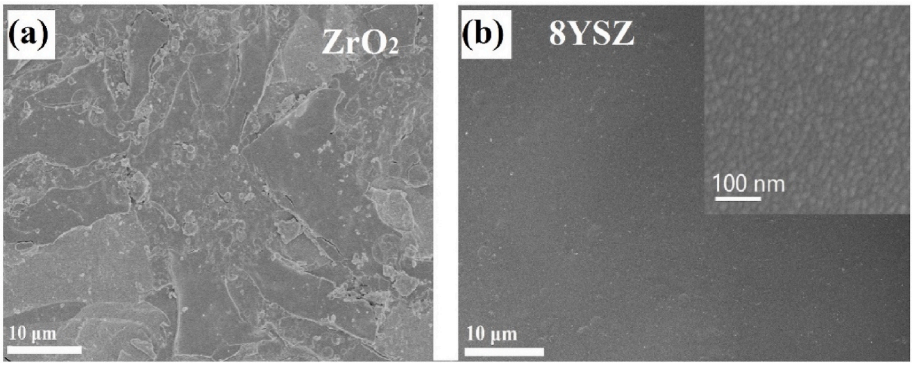

Fig. 9. Surface of NF membranes made of (a) pristine zirconia and (b) yttria-stabilised zirconia. Source: adapted from Ref. [41].

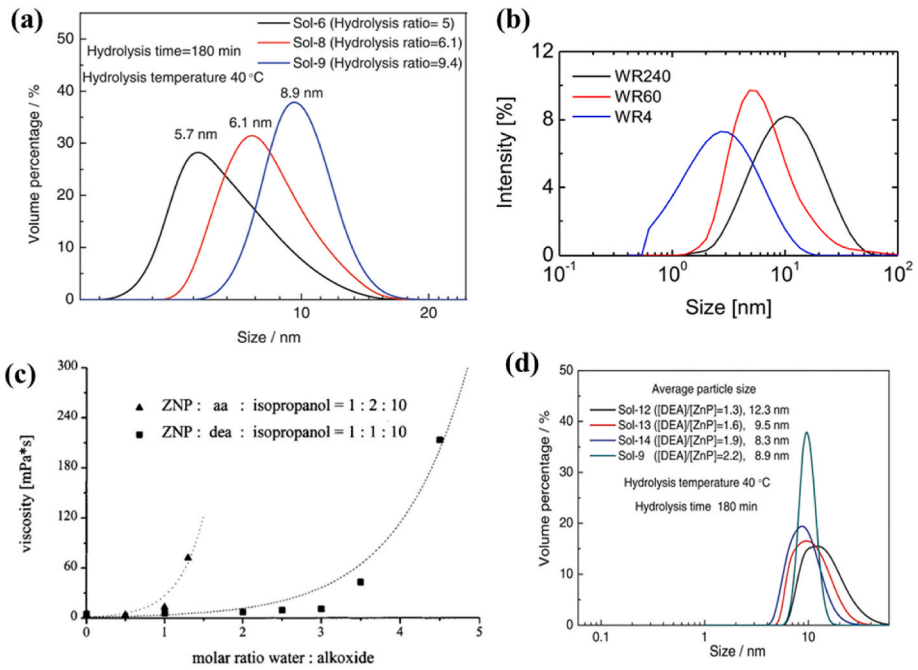

Fig. 10. (a) Effect of hydrolysis ratio on the sol particle size Source: [16]. (b) sol size at different water/alkoxide ratios Source [115]: (c) Viscosity of the gel obtained with different stabilisers Source [110]: (d) Effect of DEA ratio on gel size Source: [16].

agents, glycerol, and PEG) have been reported in the literature [37,47,109,111] for controlling the size of the gels and, consequently, the pore structure of the membrane after sintering.

Oxalic acid ($H_2C_2O_4$) has been applied as a Zr^{+4} chelating agent [31,37,47,107,157] for colloidal gels derived from inorganic zirconium salts since the organic shell around the metallic cation prevents the particles' aggregation by increasing electrostatic repulsion between them [152,160]. Da et al. [47] observed that using a molar ratio of 0.2 between oxalic acid and zirconium oxychloride ($[H_2C_2O_4]$:$[ZrOCl_2]$), the highest zeta potential was obtained, which increased the gel stability and led to the lowest sol particle size (Table 6). Similarly, with an intent to fabricate tight-UF zirconia membranes, Qin et al. [109] prepared $ZrOC_2O_4$ sols from zirconium oxychloride and oxalic acid for coating an α-Al_2O_3 support. Since the support had an average pore size of 75 nm, very large compared with the particle size, the addition of an intermediate layer prior to the top layer deposition was required. In a smart strategy, these authors prepared two colloidal gels with average particle sizes of 10 and 35 nm by varying the concentrations of precursor and oxalic acid (Fig. 11). Then, the gel with larger particles was used to spin coat the support creating a loose layer, then the gel with smaller particles was spin-coated to form a tight layer (Fig. 6b). After a sintering step, the intermediate and top layers exhibited a MWCO of 16.5 and 1 kDa, respectively.

Glycerol is another interesting additive applied in the colloidal sol-gel route owing to its several beneficial effects, including decreasing the size of the sol particles and therefore the size of the pores in the consolidated materials, increasing the specific surface area, and

Table 6
Effects of oxalic acid on the properties of colloidal sols. Source: adapted from Ref. [47].

Molar ratio of $[H_2C_2O_4]$:$[ZrOCl_2]$	pH	Zeta potential [mV]	Mean particle size of the sols [nm]
0.00:1	1.03	+1	10,000
0.15:1	0.90	+18	–
0.20:1	0.88	+36	5
0.25:1	0.87	+23	10.3
0.30:1	0.83	+22	10.8

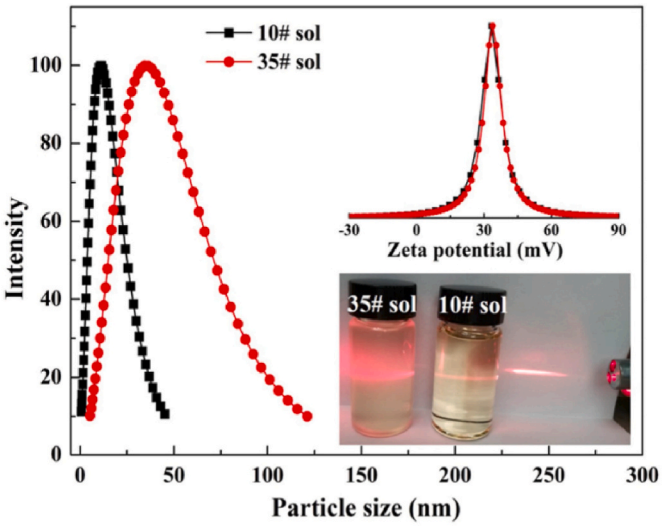

Fig. 11. Particle size distribution of $ZrOC_2O_4$ sols prepared with low (10#) and high (35#) concentration of $ZrOCl_2$ and $H_2C_2O_4$. Source: adapted from Ref. [109].

stabilizing the tetragonal phase [31,159]. These effects can be explained by the fact that glycerol bounds to the surface of the particles, thus.

(i) the electric double-layer structure is protected by inducing a steric hindrance effect, which prevents the cementation of individual particles [37]. Therefore, glycerol acts as a capping agent during the sol state [31], as illustrated in Fig. 12a;
(ii) grain rotation is inhibited, decreasing the nanoparticles packing and ordering, reducing the contact between particles, and limiting the crystal growth during drying and calcination/sintering [31].

Glycerol favours the formation of nanoparticles smaller than 10 nm, with a high surface area. In addition, more oxygen ion vacancies are

generated, which explains the stabilisation of the tetragonal phase [31] as shown in the X-ray diffractograms reported in Fig. 12b. Moreover, the addition of glycerol also allowed obtaining crack-free NF membranes as the short chains of the hydrolysed precursor can sinter without producing large voids in the layers during the firing process [37].

Similarly, Li et al. [106] employed polyethylene glycol with an average molecular weight of 6000 g mol^{-1} (PEG-6000) to improve the stability and uniformity of a colloidal sol prepared from the zirconium oxychloride, since PEG acts as a surfactant avoiding the aggregation of the sol particles.

It was also reported by some authors [135,161,162] the addition of 5–10 %wt. of α-alumina particles (average size 1–2 μm and 0.2 μm) to colloidal sols in order to prevent infiltration of the gel into the support and at the same time to smooth the support surface (Fig. 13a). The colloidal sol act as a binder for the particles [163].

In an analogue way, Bortot Coelho et al. [56] combined a Ce–ZrO_2 colloidal gel with TiO_2 P25 nanoparticles to prevent the excessive infiltration of the coating into the support (a highly porous rough SiC support with a monoclinic-ZrO_2 intermediate layer with 60 nm pore size) allowing the layer formation (Fig. 13b). As seen in Fig. 13c, the gel had a particle size of around 5 nm, and after adding the TiO_2 particles, the agglomerates had an average particle size of 250 nm. This technique allowed the authors to obtain a defect-free photocatalytic top layer with a 6 nm pore size and water permeability of 160 L m^{-2} h^{-1} bar^{-1}.

3.5. Colloidal sol-gel: Peptization

During the colloidal sol-gel process, particles with high surface energy are formed through the rapid and complete hydrolysis of the precursors in excess water. This causes the rapid growth and agglomeration of the particles, which may precipitate [164]. Therefore, the peptization process is performed to fragment these agglomerates and increase the surface charge of the particles, leading to a higher electrostatic repulsion between particles and, consequently, favouring the stability of the sol [104]. A zeta potential of at least 20–30 mV is recommended to obtain stable nanosized sols [47]. As shown in Table 7, strong acids such as nitric and hydrochloric acids [19,34] are the most commonly applied as peptising agents; however, weak acids such as acetic acid also work but in higher dosages [127,159,165], as shown in Fig. 14.

The procedure for the peptization of colloidal sols is not fully described in several works about zirconia membranes, but in general, the addition of the acid is followed by a prolonged heating period to reduce the particle size. A small compilation of the peptization conditions found in the literature is presented in Table 8.

3.6. Drying rate

Controlling the drying rate after the coating is important to avoid the formation of cracks in the deposited layer. When a wet film of colloidal particles is drying on a support, initial shrinkage occurs with solvent evaporation [167]. Then, further solvent evaporation causes the film to bind on the substrate and resists against deformations in the plane, which causes transverse tensile stresses [123]. When the magnitude of the tensile stress exceeds a critical value, cracks form spontaneously on the deposited layer [168]. Nevertheless, there is a critical thickness of the film/layer, in which, above this value, the film cracks spontaneously independent of the drying rate [167]. Since the critical crack thickness is lower for finer nanoparticles, for fabricating crack-free nanofiltration membranes, the top thickness should be even thinner than for ultrafiltration [123].

Apart from the cracks formation, uncontrolled or excessively fast drying can also lead to the loss of porosity caused by the coalescence of particles, which results in the relocation of ligands and the formation of a thin dense coating [66,169].

Therefore, the most straightforward strategy to control the drying rate is to keep the green membrane in a controlled atmosphere after coating, promoting a slow solvent removal. In Table 9, it is presented a compilation of the conditions applied in the drying of zirconia gels, usually in temperatures below 100 °C for colloidal gels and at room temperature (RT) for polymeric ones.

In the colloidal sol-gel route, since the solvent is usually water, a low drying temperature and higher relative humidity are enough to control the drying rate [34,107]. However, in many cases, the organic additives used as binders and plasticisers, such as polyvinyl alcohol and polyethylene glycol, also slow down the drying rate [123]. These additives are discussed in the next section. In the case of the polymeric route, the sol is prepared in organic solvents with higher vapour pressures (*e.g.,* propanol, hexane), but usually, the stabiliser of the precursor (*e.g.,* DEA) also acts to control the gel drying.

3.7. Binders

A temporary binder, usually a natural or synthetic polymer, has many functions: adjust the sol (coating fluid) viscosity; control the degree of infiltration of the coating into the support; increase the mechanical stability of the green body (membrane layer before sintering) by temporary binding them to each other and to the support; prevent flocculation of the sol; and lower the sol surface tension [56,122,172]. In most works published about ZrO_2 membranes (Table 10), polyvinyl alcohol (PVA) is used as a binder, which is totally burned off during the sintering. Some organic binders like PVA and polyethylene glycol (PEG) also prevent the crack formation in the initial drying process [173].

Qiu et al. [123] investigated the influence of the PVA, PEG, and methylcellulose (MC) binders on the drying rate and crack formation for obtaining crack-free zirconia membranes. These authors reported that MC had a more substantial effect on viscosity increase, while PVA was more effective in increasing the critical thickness and preventing crack-formation (Fig. 15).

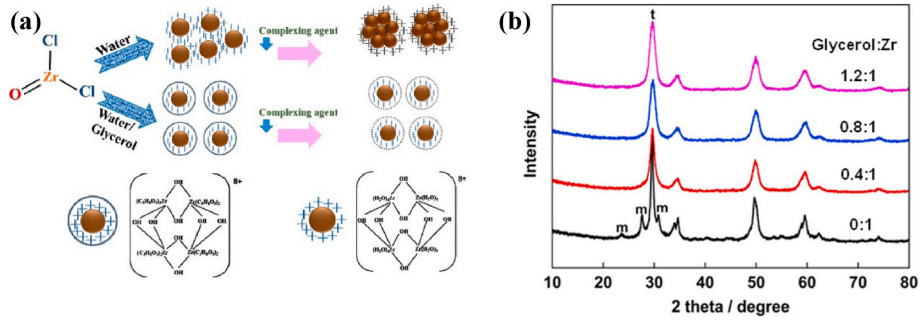

Fig. 12. (a) Effects of glycerol in the formation of colloidal ZrO_2 sol from $ZrOCl_2$. Source: [31]; (b) X-ray patterns of gels prepared with different amounts of glycerol after calcination at 400 °C, indicating the monoclinic (m) and tetragonal (t) ZrO_2 phases. Source: adapted from Ref. [31].

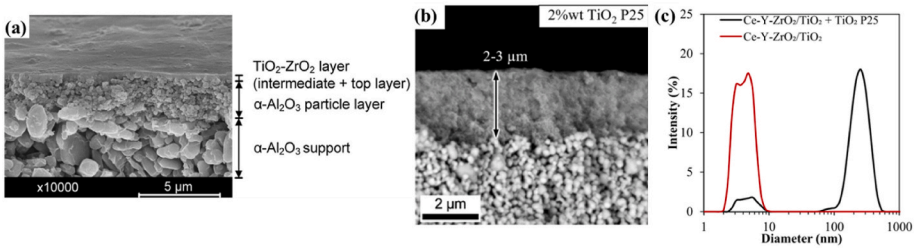

Fig. 13. (a) Cross-section of the asymmetric membrane with the α-alumina particle layer coated with colloidal sol as a binder. Source: [135]; (b) cross-section of Ce–Y–ZrO_2/TiO_2 layer on ZrO_2 intermediate layer, (c) particle size distribution of sol (Ce–Y–ZrO_2/TiO_2) and coating fluid (Ce–Y–ZrO_2/TiO_2 + TiO_2 P25). Source: adapted from Ref. [56].

Table 7
Test of different acids to peptise an alumina sol. Source: [166].

Acid	Formula	Result after 7 days
Nitric	HNO_3	Clear sol
Hydrochloric	HCl	
Perchloric	$HClO_4$	
Acetic	CH_3COOH	
Trichloroacetic	CCl_3COOH	
Monochloroacetic	$CH_2ClCOOH$	Clear sol to cloudy
Formic	HCOOH	
Oxalic	$H_2C_2O_4.2H_2O$	
Hydrofluoric	HF	Unpeptized
Iodic	HIO_4	
Sulfuric	H_2SO_4	
Phosphoric	H_3PO_4	
Boric	H_3BO_4	
Phthalic	$C_8H_4O_3$	
Citric	$H_3C_6H_5O_7.H_2O$	
Carbolic	C_6H_5OH	

3.8. Sintering

The final stage of the zirconia membrane fabrication is carried out through a multistep thermal treatment, as illustrated in Fig. 16a. The first sintering step, in the presence of oxygen (usually air atmosphere) and at lower temperatures, is set to eliminate the organic groups in the dried gel (*e.g.,* organic groups of the precursor, binders, additives) and to form zirconium oxide. The average temperature for obtaining a pure inorganic membrane depends on the composition of the gel, but it has been reported in the literature between starting from 300 to 350 °C [127]. A second step, at higher temperatures, is carried out to promote particles' consolidation (development of necks that weld the particles to one another), densification (reduction of the porosity, shrinkage of the whole body), and grain coarsening (increase in the size of the particles and the grains) [172], as schematised in Fig. 16b. The sintering conditions substantially affect the final membrane properties, including pore size distribution (Fig. 16c), morphology, zeta potential, crystallisation, and phase transformation [174].

For pure ZrO_2 gels sintered below 350–400 °C, no crystalline phase is observed in the XRD analysis indicating the formation of an amorphous zirconia phase [135,175]. Qi et al. [16] observed that by increasing the sintering temperature from 350 to 400 °C, the MWCO of the membrane increased from 354 to 1195 Da. Consequently, the pure water permeability also increased from 20 to 30 L m^{-2} h^{-1} bar^{-1} (Fig. 17a), probably because of the ZrO_2 crystallisation accompanied by particle growth and pore opening.

For sintering temperatures between 400 and 500 °C, sol-gel-derived ZrO_2 forms preferably the tetragonal polymorph [176]. Sintering temperatures in this range were reported in a significant part of NF zirconia membranes works [31,34,41,108–111]. Higher temperatures would lead to grain growth, an increase in pore size (Fig. 16c), and the transformation to the monoclinic phase (Fig. 17b), which cause cracks on the layer (Fig. 17c) due to the volume variation involved in this transformation [13,35]. Erdem [133] observed that the magnitude of the zeta potential increased linearly (~32%) in the 400–500 °C range because of the tetragonal to monoclinic phase transformation.

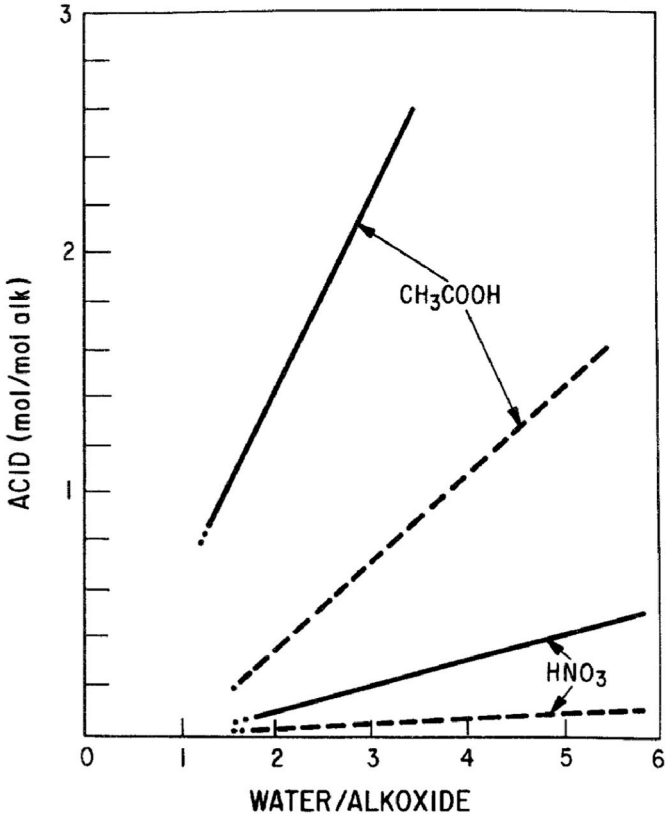

Fig. 14. Amount of acid required to obtain clear sols as a function of water/alkoxide ratio at two different solution concentrations of hydrolysed Zr $(OC_3H_7)_4$ in propanol. (—) 5% weight equivalent ZrO_2, (–) 2.5% weight equivalent ZrO_2. Source: [165].

Concerning the effect of the sintering temperature on membrane stability, it is known that a crystalline material usually has higher chemical stability than an amorphous one [88], which may be preferred for special applications under corrosive conditions and higher temperatures (*e.g.* in gas separation). Therefore, sintering at temperatures higher than the crystallisation temperature can favour stability but leads most of the time to larger pore sizes [16,22,135]. Similarly, Puthai et al. [24] observed that the Si and Zr solubilities in water are higher for SiO_2–ZrO_2 membranes sintered at 200 °C than the ones sintered at 550 °C. Moreover, temperature can affect mechanical properties. For instance, when 3YSZ was used for fabricating a zirconia membrane on SiC supports (flexural strength 25 MPa), the increase in the sintering

Table 8
Conditions reported for the peptization of colloidal zirconia sols.

Precursor	Acid	Molar ratio Zr:Acid	Temperature [°C]	Time [hours]	Reference
$ZrOCl_2$	Oxalic	1:0.2	80	3	[47]
$Zr(OC_4H_9)_4$	Hydrochloric	1:(1.5–6)	Boiling	9	[139]
$ZrOCl_2$	Nitric	1:1	40	24	[106]
$Zr(OC_4H_9)_4$ $Ti(OC_3H_7)_4$	Hydrochloric	1:5.6	25 Boiling	12 + 8	[135]

Table 9
Additives and drying conditions for sol-gel processes applied in the fabrication of ZrO_2 membranes.

Sol-gel route (Solvent)	Additives	Drying Conditions	Drying time (h)	Reference
Colloidal (Water)	Glycerol PVA	60 °C 60 %RH	12	[31,47]
	PVA	RT	12	[107]
	PEG-6000	(i) RT (ii) Muffle at 100 °C	12 2	[106]
	Glycerol PVA	60 °C 60 %RH	12	[37]
	HPC PVA	40 °C 60 %RH	3	[170]
	PVA	40 °C 60 %RH	–	[34]
Polymeric (Propanol)	acac	Air	–	
	DEA	Air	72	[110]
	DEA	Air 4 °C	72	[50]
	DEA	Air	12 h	[171]

RT: room temperature, RH: relative humidity, acac: acetylacetone, PVA: polyvinyl alcohol, DEA: diethanolamine, HPC: hydroxypropyl cellulose.

Table 10
Selected works on the fabrication of zirconium membranes, with the binders utilised in each one, separated by the sol-gel route applied and the final pore size obtained.

Sol-gel route	Precursor	Binder (Additive)	Top Layer Thickness (nm)	Pore size (nm)	Reference
Colloidal	$ZrOC_2O_4$	PVA	180 100	1.3 1.4	[31,111]
		Tween 80	200	1.6	[109]
		PVA	150	4	[107]
	Zr-PR/Ti-PR	PVA	3000	6	[56]
	$Zr(NO_3)_4$ Ti-BT	PVA	200	1.5	[37]
	Ti-iPR ZrO $(NO_3)_2$	HPMC, PVA	1000	3–10	[170]
	$ZrOCl_2$	PEG-6000	63,000	65	[106]
Polymeric	Zr-PR	No additive	50	(<300 Da)	[34]
		(DEA)	100	1–2	[108]
		(DEA)	50	1–2	[110]
		PEG (DEA, Glycerol)	260	1.4	[41]
	Zr-PR/Ti-PR	(DEA)	90	1.2–.15	[116]

PVA: polyvinyl alcohol, PEG: polyethylene glycol, DEA: diethanolamine, HPMC: hydroxypropyl methylcellulose, Zr-PR: zirconium propoxide, Ti-PR: titanium propoxide, Ti-iPR: titanium isopropoxide.

temperature from 800 to 1000 °C led to a higher flexural strength (from 28 to 38 MPa) own to the higher proportion of the tetragonal polymorph, which has higher mechanical and chemical stabilities [114].

As discussed previously, zirconia doping with yttrium can stabilise the tetragonal polymorph, allowing higher sintering temperatures up to 700 °C without monoclinic phase formation [19,175]. The addition of titanium to create mixed ZrO_2–TiO_2 oxides affects the crystallisation temperature and the phase behaviour, which will be discussed in a further section.

For UF zirconia membranes fabricated by sol-gel processes, higher sintering temperatures need to be applied to ensure the layer's mechanical stability and adhesion to the support, which has large pores. Li et al. [106,114] studied the sintering of ZrO_2 layers on SiC supports at temperatures from 600 to 1000 °C. In both works, zirconia particle size increased with the increase in temperature. As the sintering temperature increased from 800 to 1000 °C, the average size of zirconia grains practically doubled since the growth of zirconia particles is controlled by the diffusion and migration of grain boundaries, which are enhanced at a higher temperature. The average pore size of the top layer reduced from 63 nm at 700 °C to 48 nm at the sintering temperature of 900 °C [106], and from 82 nm at 800 °C to 54 nm at 1000 °C [114], caused by the densification of the zirconia particles (Fig. 18). As a result of the pore size decline, the water permeability also decreased for higher sintering temperatures. On the contrary, Larbot et al. [104] observed that between 470 and 720 C, the pore diameters do not vary while the crystalline structure is tetragonal. Above 720 °C, the monoclinic structure appears, and the pore diameters increase from 3 to 80 nm (Fig. 16c), as well as the water permeability.

3.9. Mixed oxides (ZrO_2–SiO_2 and ZrO_2–TiO_2)

Combining ZrO_2 with other oxides, such as TiO_2 and SiO_2, brings advantages in the synthesis process and the membrane properties. Table 11 presents selected works on ZrO_2–SiO_2 and ZrO_2–TiO_2 membranes.

Silica (SiO_2) is a widely studied material for the fabrication of meso- and microporous ceramic membranes by sol-gel processes [127,154], owing to its great advantage in terms of pore-size controllability [14, 178]. For example, Darmawan et al. [179] fabricated a hydrophobic SiO_2 membrane for desalination with more than 99% of salt rejection. Nevertheless, amorphous silica is an acidic metal oxide that has often been reported to be unstable in aqueous solutions, especially at high temperatures [161]. Furthermore, SiO_2 gradually dissolves in neutral or alkaline media, significantly decreasing the lifetime of the membrane [180].

Therefore, the combination of silica and zirconia can increase the stability of the membrane in aqueous solutions. Puthai et al. [24] prepared SiO_2–ZrO_2 NF membranes in a porous α-Al_2O_3 support. Tetraethoxysilane (TEOS) and zirconium-tetra-butoxide were used to prepare different colloidal sols with Si/Zr molar ratios of (1/0, 9/1, 7/3, 5/5, 3/7, 0/1). The obtained membranes were tested for hydrothermal stability and corrosion resistance at pH values of 2 and 12, even though no corrosion was observed in acid media. As a result, high dissolution of Si was observed in water at 90 °C and basic environment for the compositions with low Zr content. However, higher molar ratios of Zr prevented Si from dissolving and favoured the formation of hydroxyl groups that enhanced membrane hydrophilicity and the rejection of the selective layer. Similarly, TEOS and zirconium propoxide/butoxide were applied as percussor for fabricating reverse osmosis [181] and nanofiltration membranes [161] in a range of 0.8–2.5 nm. The MWCO values obtained for the SiO_2–ZrO_2 membranes were smaller than those of γ-Al_2O_3 and TiO_2 [14], while the incorporation of zirconia into silica

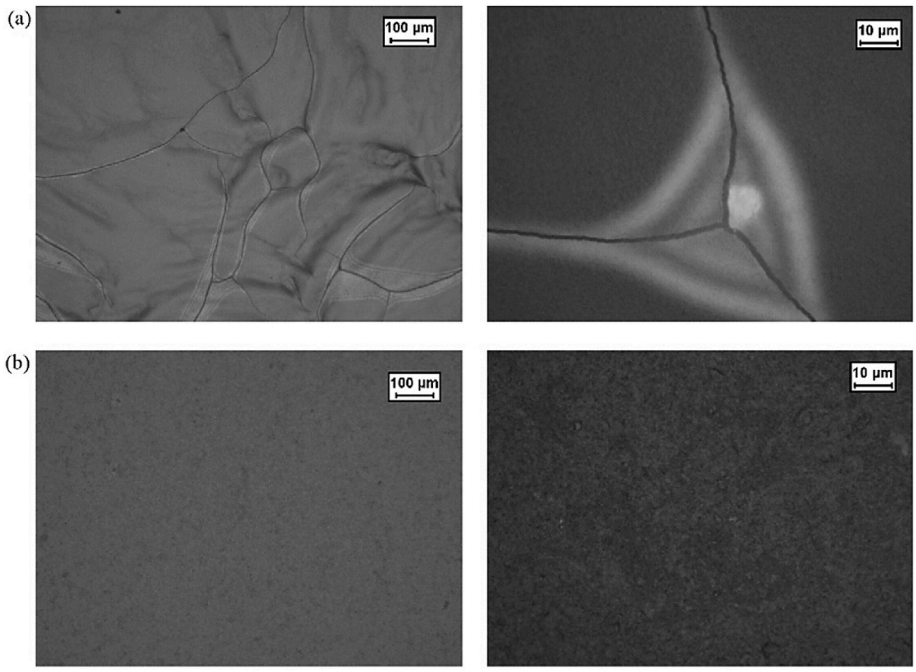

Fig. 15. SEM images of the dried films cast on a glass substrate with (a) no binder; (b) PVA. Source: adapted from Ref. [123].

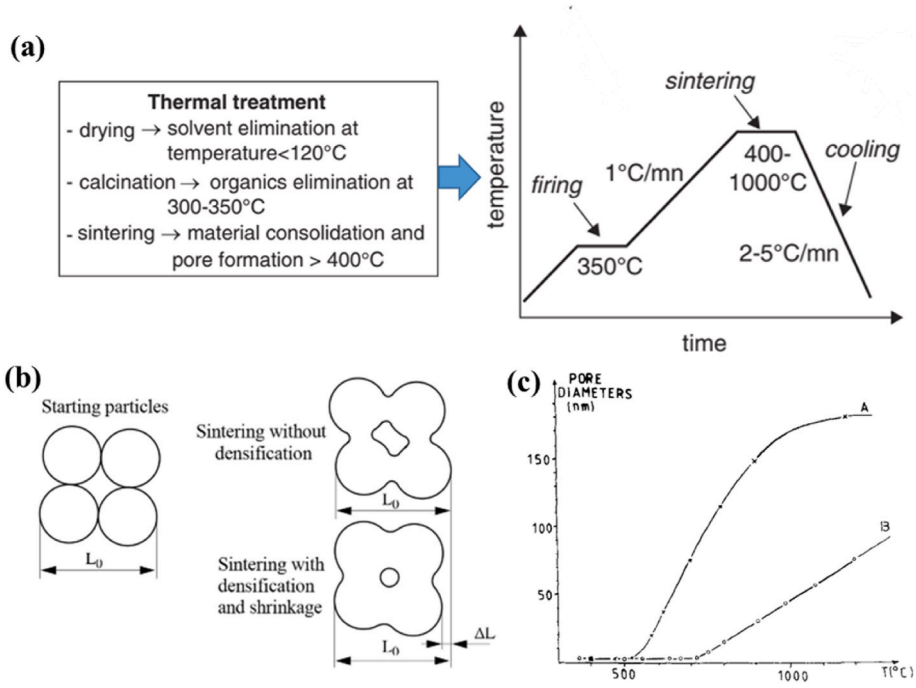

Fig. 16. (a) generic thermal treatment process. Source: adapted from Ref. [127], (b) representation of densifying and non-densifying sintering mechanisms. Source: adapted from Ref. [172]; (c) pore size as a function of sintering temperature for A: TiO_2 membranes B: ZrO_2 membranes. Source: adapted from Ref. [104].

improved the stability in aqueous solutions. Lawal et al. [115] prepared a carbon-SiO_2-ZrO_2 composite membrane for gas separation with pores below 1 nm. With a Si/Zr ratio of 9/1, a high level of H_2 permselectivity was obtained, allowing H_2/N_2 and H_2/CH_4 separation.(See. Fig. 19)

Regarding titania, it presents similar mechanical, thermal, and chemical properties compared to zirconia, making it an excellent material for ceramic membranes [182]. However, the practical application of TiO_2 in separation layers is limited by the reduction of porosity and crack formation in the partial anatase to rutile phase transformation that occurs upon sintering at temperatures higher than 350 °C [130]. Similarly, pure ZrO_2 membranes can also crack during sintering because of large volume variation (~4–9%) in their monoclinic/tetragonal phase transformation [13]. In addition, TiO_2 and ZrO_2 amorphous to crystalline phase transformation around 350 and 400 °C, respectively, is accompanied by the growth of grain and pore sizes [135].

Therefore, combining TiO_2 and ZrO_2 can increase zirconia crystallisation temperature up to 700 °C and stabilise its tetragonal polymorph [50,176], depending on the Zr/Ti molar ratio (Fig. 20a). The TiO_2 addition leads to forming a solid solution with ZrO_2 for compositions containing less than 40% of TiO_2 [50], with the preferred phase being a

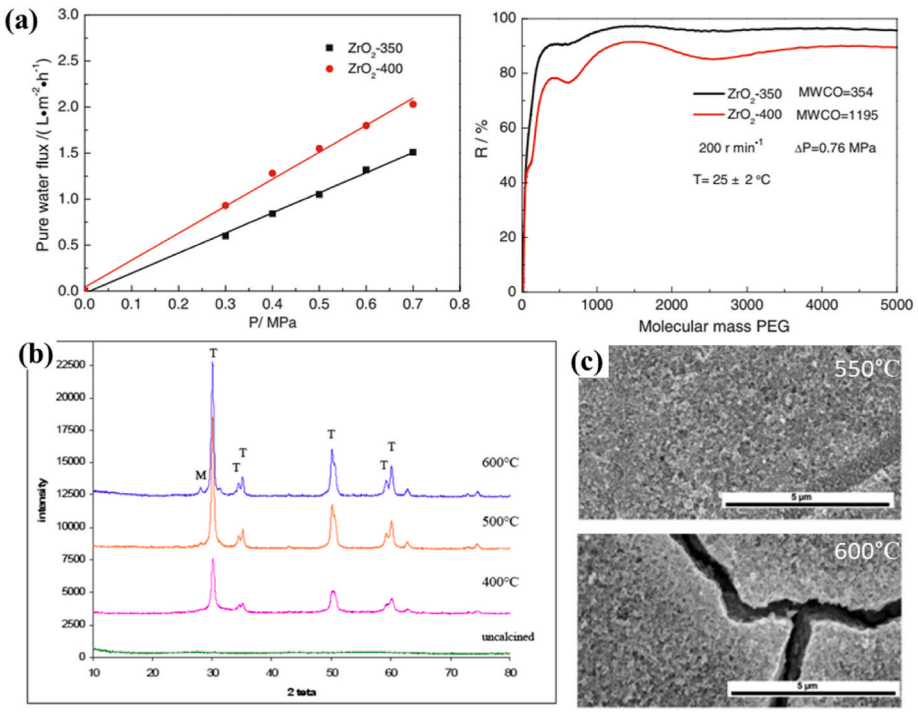

Fig. 17. (a) water permeability and MWCO for ZrO2 membranes sintered at 350 and 400 °C. Source: adapted from Ref. [16]; (b) XRD analysis of ZrO_2 unsupported membrane sintered at different temperatures. Source: adapted from Ref. [177]; (c) crack formation in the top layer caused by higher sintering temperature. Source: adapted from Ref. [56].

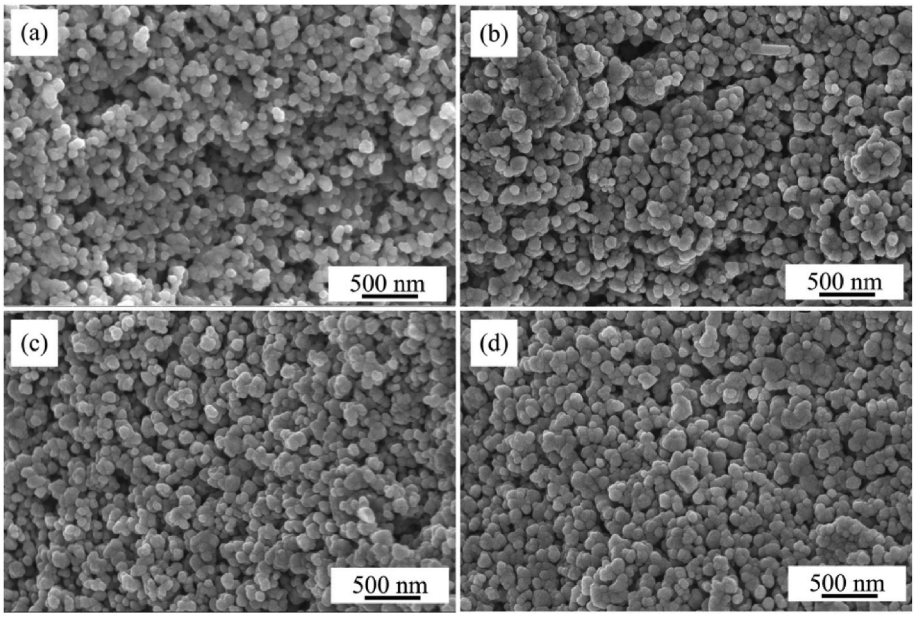

Fig. 18. Morphology of ZrO_2 top layer (on top of SiC supports) obtained with the sintering temperatures of: (a) 800 °C, (b) 900 °C, (c) 950 °C, (d) 1000 °C. Source: [114].

greatly disordered ZrO_2 tetragonal phase [176]. For these Zr-rich oxides, the TiO_2 addition reduces sol particle size [37], which after sintering leads to smaller crystallite sizes [177], higher porosities [176] and surface areas [37] (Fig. 20b–d). In the range of 40–70% TiO_2, it is formed the orthorhombic compound $ZrTiO_4$, which has crystallisation temperatures of nearly 700 °C, but with lower surface area and porosity [176]. Nevertheless, this material was applied to fabricate amorphous nanofiltration membranes with MWCO as low as 265 Da and satisfactory hydrothermal stability [88,183], and NF membranes with MWCO between 620 and 860 Da [116] by dip-coating γ-alumina disks (pore size: 5–6 nm) with a polymeric sol-gel and sintering them at 400 °C. Furthermore, the combination of ZrO_2 and TiO_2 can also be useful in tuning the membrane's zeta-potential [177] or increasing the photocatalytic activity of TiO_2 [130,184].

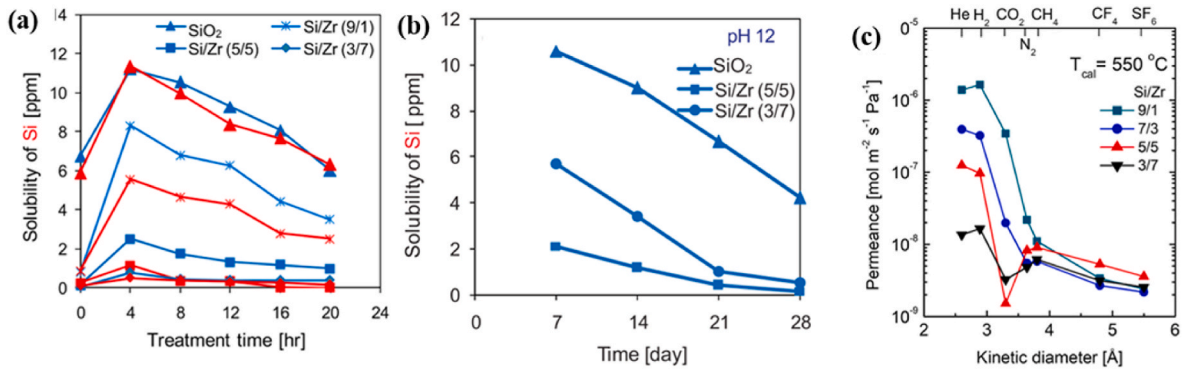

Fig. 19. Solubility of Si in SiO_2–ZrO_2 membranes in (a) hydrothermal conditions (b) basic media. Source: adapted from Ref. [24]; (c) Single-gas permeance at 200 °C as a function of the kinetic diameter of carbon-SiO_2–ZrO_2 derived membranes. Source: adapted from Ref. [115].

Table 11
Main works on zirconia mixed oxides membranes.

Material	Type	Sintering Temp. (C)	Support (Pore size)	Phase	Water permeability (LMH/bar)	Pore size (nm)	Reference
ZrO_2–SiO_2	NF	570	α-Al_2O_3 (1000 nm)	–	0.5	1–3	[161]
		200/550	α-Al_2O_3	Amp	1	0.6	[24]
	Gas separation	300, 550	Al_2O_3 + SiO_2–ZrO_2	Amp/T	–	0.2	[115]
		250–550	α- Al_2O_3 (1200 nm)	Amp/T	–	<1	[162]
ZrO_2–TiO_2	UF	400–700	SiC (5 μm) + ZrO_2 (60 nm)	T	160	6	[42,56]
		500	α-Al_2O_3 + TiO_2	A	5	4	[130]
		450–700	α-Al_2O_3 (100 nm)	A	3.5	3.6	[170]
	NF	400	α-Al_2O_3 + γ- Al_2O_3 (5–6 nm)	Amp	<1	1.3	[116]
		550	α- Al_2O_3 (2100 nm) + Al_2O_3/TiO_2–ZrO_2 (1.5 nm)	Amp	0.7–4	<1	[135]
		500	TiO_2 (10 nm)	T	35	1.5	[37]
		550	α-Al_2O_3 (60 nm) + ZrO_2 (3.5 nm)	T	10	1.3	[50]
	Gas separation	350–500	α- Al_2O_3 (100 nm) + SiO_2–ZrO_2	Amp	–	<1	[67]

Amp: amorphous phase, T: tetragonal ZrO_2, LMH/bar: L m^{-2} h^{-1} bar^{-1}.

4. Fabrication of ZrO_2 membranes by molecular layer deposition (MLD)

Atomic Layer Deposition (ALD) and Molecular Layer Deposition (MLD) on planar non-porous substrates, ALD [185–189] and MLD [190,191] are well-known deposition techniques to deposit films with (sub-) monolayer thickness control [192–195].ALD is limited to inorganic precursors, while MLD is extended to organic substances and makes it possible to link both types of building blocks together in a controlled manner to build organic-inorganic hybrid materials. Both ALD and MLD are depositions in a vapour phase based on sequential self-limiting surface reactions. Typical is the use of sequential self-limiting surface AB half-reactions to achieve uniform and conformal films even on complex 3D topologies. This makes the technique very interesting for membrane application [196].

A two-step MLD reaction between a metal alkyl, such as trimethylaluminum (TMA), and a diol, such as ethylene glycol (EG), can be written in general as follows [197,198]:

$$SR'OH^* + MR_x \rightarrow SR'O{-}MR_{x-1}^* + RH \quad (3)$$

$$SMR^* + HOR'OH \rightarrow SM{-}OR'OH^* + RH \quad (4)$$

The asterisks indicate the surface species, and S denotes the substrate with the reaction products from the previous reactions. The first reaction (Eq. (3)), called A reaction, stops when all the SR′OH* species have completely reacted with precursor 1 (MR_x) to produce $SR'O{-}MR_{x-1}$. After a nitrogen purge, precursor 2 (HOR′OH) is introduced in the reaction media, and the second reaction (Eq. (4)), called B reaction, stops when all the SMR* species have completely reacted to produce SM-OR. The sequential self-limiting reactions of, in this case, TMA and EG ideally yield a metal alkoxide polymeric film described by (Al–(O–CH_2–CH_2–O–)) linkages.

In recent literature, molecular layer deposition was used to prepare TiO_2 nanofiltration membranes for water purification (Fig. 21) [190]. After the deposition, the organic part was de-binded, resulting in a pore with approximately 1 nm diameter. The membrane showed a pure water permeability as high as ~48 L m^{-2} h^{-1} bar^{-1}. Salt and dye rejection measurements showed moderate rejection of Na_2SO_4 (43%) and $MgSO_4$ (35%) and high rejection of methylene blue (~96%). Wang et al. showed that the choice of the calcination temperature could tune the pores of the resulting TiO_2 membranes. Changing the temperature from 250 to 400 °C resulted in an increase in the molecule weight cut-off (MWCO) from 630 Da (Nanofiltration range) to 3000 Da (tight Ultrafiltration range) [8].

To our knowledge, zirconia MLD film has only deposited on dense support. Still, the hybrid organic-inorganic MLD films might be interesting as the metal oxide, ZrO_2, has a high dielectric constant and a high refractive index and could be interesting for their optical and antimicrobial coatings. George et al. [199] showed linear growth using zirconium tetra-tert-butoxide (ZTB) and ethylene glycol (EG). In Fig. 22, a scheme shows the binary reaction sequence for zirconia MLD film growth using ZTB and EG. They reported a confirmed linear growth at 145 °C with a growth rate of 0.8 Å per MLD cycle. In 2021, Rogowska et al. [200] reported that photoactive organic molecules could be combined with biocompatible metals like Zr or Ti to create antimicrobial

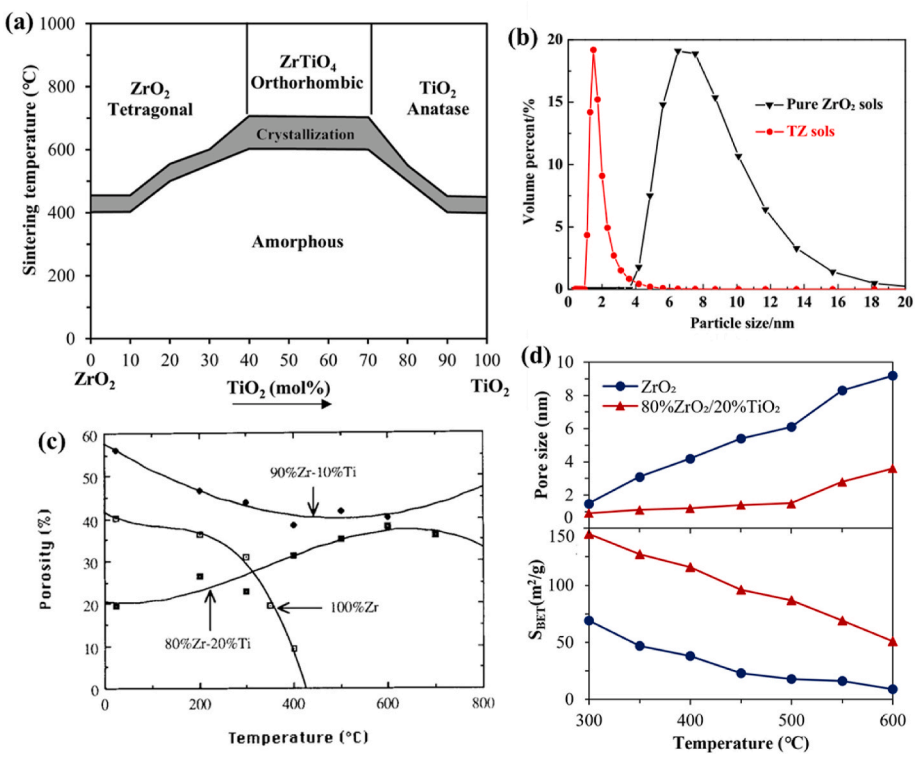

Fig. 20. (a) Phase diagram of ZrO_2–TiO_2. Source: elaborated with data from Refs. [50,176]; (b) particle size distribution for pure ZrO_2 and ZrO_2–TiO_2 (TZ) sols. Source: [37]; (c) Porosity of fired gels as a function of calcination temperature. Source: [176]; (d) pore size and specific surface area (S_{BET}) of ZrO_2–TiO_2 unsupported membranes. Source: elaborated with data from Ref. [37].

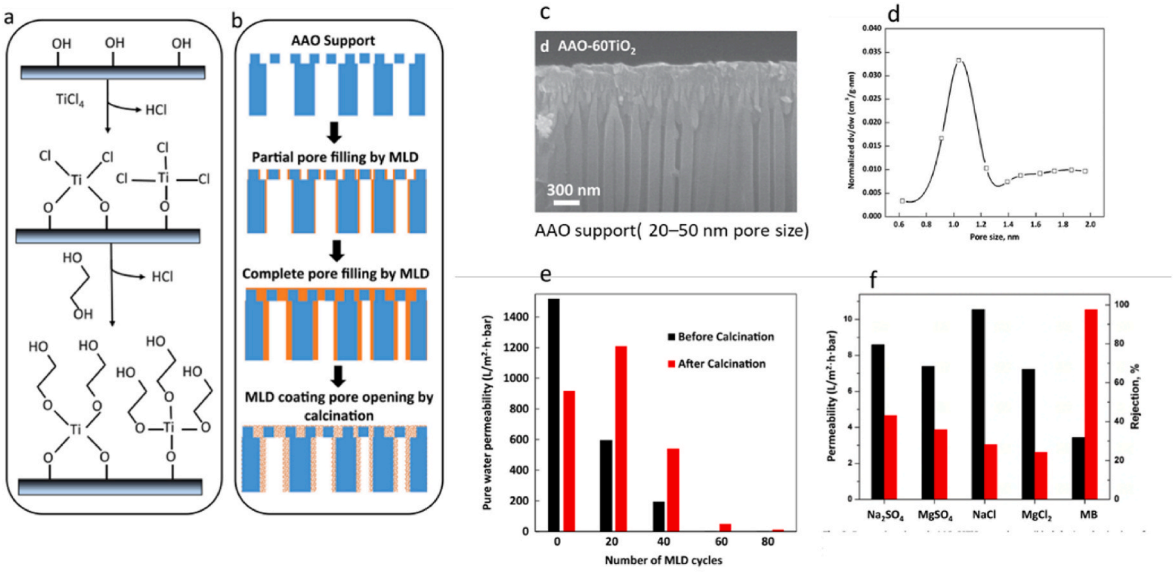

Fig. 21. MLD deposition of TiO_2 (a) Schematic diagrams of MLD surface reactions, (b) step-by-step procedure to prepare the TiO2 nanofiltration membrane, (c) SEM image of the membrane, (d) pure water permeation after calcination at 250 °C, (e) permeation throught the membrane. Source: adapted from Ref. [190].

coatings. Those examples show that the application of Zirconia might be interesting for specific membrane applications.

5. Conclusion and future perspectives

The present paper presented a critical review of the progress in the fabrication of UF and NF zirconia membranes, including the current state of the commercially available ZrO_2 membranes and the recent innovations in academia. This work is unique in reviewing zirconia membranes and therefore fills a gap in the literature, being a guide for beginners in the field and established researchers. Although the significant advances in the fabrication and applications of ZrO_2 membranes, there are some critical points for future research and developments.

1) Most commercialised zirconia membranes are for MF and UF [2,10, 15], own to the challenges in obtaining defect-free NF,

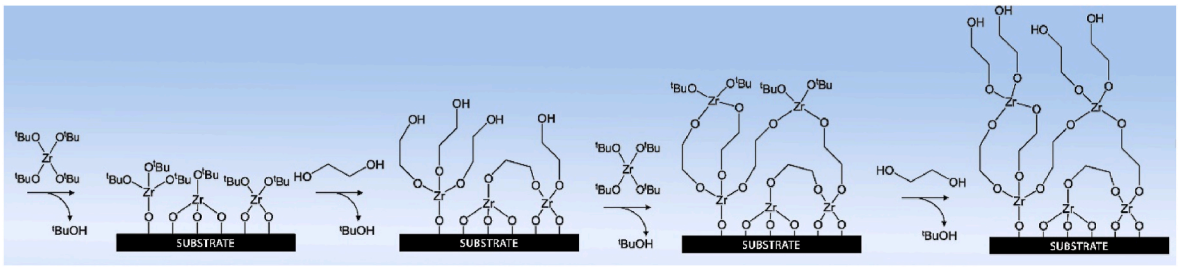

Fig. 22. Reaction sequence for zirconia MLD film growth using zirconium tetra-tert-butoxide (ZTB) and ethylene glycol (EG). Source: adapted from Ref. [199].

pervaporation, and gas separation membranes. The present work reviewed several techniques proposed by different authors to overcome these challenges, such as Y-doping and mixing with TiO_2 or SiO_2. Nevertheless, to increase the industrial use of the membranes developed in the academic setting, it is necessary to do more research and development on up-scaling the fabrication techniques into industrial processes to make NF, pervaporation, and gas separation ZrO_2 membranes more cost-effective.

2) Membrane filtration processes are currently dominated by polymeric membranes, which have a limited lifetime. However, ZrO_2 membranes have great potential to replace them in applications requiring high stability, such as desalinization, protein recovery, and complex separations in pharmaceutical and metallurgy industries. Therefore, zirconia membranes should be applied in new processes where filtration was not feasible, including extreme acid and basic feeds (*e.g.,* acid mine drainage, black liquor from the paper industry), solvent filtration, and feeds at high temperatures or high pressure.
3) The sol-gel coating is the most applied method for fabricating microporous ZrO_2 membranes, offering great flexibility in the synthesis and process parameters for tunning the final membrane properties. A significant development was observed with the adequate stabilisation of the zirconia precursors, controlling their rapid hydrolysis and condensation reactions, which allowed obtaining membranes with pore size below 1 nm with elevated hydrothermal resistance. In addition, support selection and strategies to avoid the excessive infiltration of the coating into the support can reduce the layer thickness, ensuring a small pore size and a relatively high water permeability without losing the selectivity.
4) Combining ZrO_2 with other oxides, such as SiO_2 and TiO_2, can increase stability and promote the formation of pores below 1 nm can be obtained, allowing H_2/N_2 and H_2/CH_4 separation [115]. In addition, the crystallisation temperature can be increase up to 700 °C [50,176], and be used to fabricate amorphous NF membranes with MWCO as small as 265 Da [88,183]. Mixed oxide zirconia membranes can also be useful for tuning the membrane's zeta-potential [177] or increasing the photocatalytic activity of TiO_2 [130,184].
5) Most of the papers on microporous ZrO_2 membranes report as characterisation and testing, only measurements of clean water permeability and PEG (or dextran) retention to calculate MWCO and estimate the pore size. A limited number of works present corrosion tests and the retention of salts, pesticides, and dyes. Further research is necessary to explore the performance of ZrO_2 membranes on a pilot scale and long-term filtration tests under actual industrial conditions, or using as feed, real wastewaters.

Considering the challenges uprising with climate change and the actions to avoid it while preserving the environment, it is necessary to implement more sustainable production processes and more effective wastewater treatments. The advances in high-performing and durable zirconia membranes can contribute to more efficient and greener processes, reducing tails, and promoting water reuse, which could contribute to reducing environmental impact and carbon emissions while helping to achieve the UN's Sustainable Development Goals (SDGs): Clean water and Desalination (Goal 6), Life below the water (Goal 14), and Responsible consumption and production (Goal 12), since ceramic membranes help the transition towards a circular economy.

Declaration of competing interest

The authors declare that they have no known competing financial interests or personal relationships that could have appeared to influence the work reported in this paper.

Acknowledgements

This paper is part of the $PH_2OTOclean$ project that has received funding from the Innovation Fund Denmark under the research and innovation scheme Industrial Postdoc 2021, case number 1045-00014B.

Nomenclature

A	Anatase TiO_2
acac	Acetylacetone
AOM	Algal organic matter
BSA	Bovine serum albumin
C	Colloidal sol-gel route
CEC	Contaminants of emerging concern
CNTs	Carbon nanotubes
CVD	Chemical vapour deposition
DEA	Diethanolamine
EG	Ethylene glycol
HA	Humic acid
HPC	Hydroxypropyl cellulose
HPMC	Hydroxypropyl methylcellulose
HR	Hydrolysis ratio
LMH/bar	$L\ m^{-2}\ h^{-1}\ bar^{-1}$
M	Monoclinic ZrO_2
MC	Methylcellulose
MF	Microfiltration
MLD	Molecular Layer Deposition
MW	Molecular Weight
MWCO	Molecular Weight Cut-off
NF	Nanofiltration
P	Polymeric sol-gel route
PEG	Polyethylene glycol
PV	Pervaporation
PVA	Polyvinyl alcohol
RH	Relative humidity
RO	Reverse osmosis
RT	Room temperature
SDGs	Sustainable Development Goals
T	Tetragonal ZrO_2
TEOS	Tetraethoxysilane
Ti-BT	Titanium (iv) butoxide
Ti-iPR	Titanium (iv) iso-propoxide
TMA	Trimethylaluminum

UF	Ultrafiltration
WW	Wastewater
XRD	X-ray diffraction analysis
YSZ	Yttria Stabilised Zirconia ~ 3YSZ and 8YSZ
Zr	Zirconium
ZrO_2	Zirconia, Zirconium Dioxide
ZrPR	Zirconium (iv) propoxide (or iso-propoxide or n-propoxide)
ZrTB	Zirconium (iv) tert-butoxide

References

[1] W. Liu, X. Liu, H. Yang, P. Ciais, Y. Wada, Global water scarcity assessment incorporating green water in crop production, Water Resour. Res. 58 (2022), https://doi.org/10.1029/2020WR028570.

[2] Z. He, Z. Lyu, Q. Gu, L. Zhang, J. Wang, Ceramic-based membranes for water and wastewater treatment, Colloids Surfaces A Physicochem. Eng. Asp. 578 (2019), 123513, https://doi.org/10.1016/j.colsurfa.2019.05.074.

[3] T. Nawaz, S. Sengupta, Contaminants of emerging concern: occurrence, fate, and remediation, in: Adv. Water Purif. Tech., Elsevier, 2019, pp. 67–114, https://doi.org/10.1016/B978-0-12-814790-0.00004-1.

[4] E.A. Serna-Galvis, A.M. Botero-Coy, D. Martínez-Pachón, A. Moncayo-Lasso, M. Ibáñez, F. Hernández, R.A. Torres-Palma, Degradation of seventeen contaminants of emerging concern in municipal wastewater effluents by sonochemical advanced oxidation processes, Water Res. 154 (2019) 349–360, https://doi.org/10.1016/j.watres.2019.01.045.

[5] S. Kim, K.H. Chu, Y.A.J. Al-Hamadani, C.M. Park, M. Jang, D.-H. Kim, M. Yu, J. Heo, Y. Yoon, Removal of contaminants of emerging concern by membranes in water and wastewater: a review, Chem. Eng. J. (2017), https://doi.org/10.1016/j.cej.2017.11.044.

[6] J.M. Gohil, P. Ray, A review on semi-aromatic polyamide TFC membranes prepared by interfacial polymerization: potential for water treatment and desalination, Separ. Purif. Technol. 181 (2017) 159–182, https://doi.org/10.1016/j.seppur.2017.03.020.

[7] M. Essalhi, M. Khayet, Fundamentals of membrane distillation, in: Pervaporation, Vap. Permeat. Membr. Distill., Elsevier, 2015, pp. 277–316, https://doi.org/10.1016/B978-1-78242-246-4.00010-6.

[8] P. Hadi, M. Yang, H. Ma, X. Huang, H. Walker, B.S. Hsiao, Biofouling-resistant nanocellulose layer in hierarchical polymeric membranes: synthesis, characterization and performance, J. Membr. Sci. 579 (2019) 162–171, https://doi.org/10.1016/j.memsci.2019.02.059.

[9] Zhou Yang, Rui Feng, Zhang Zhang, A review on reverse osmosis and nanofiltration membranes for water purification, Polymers 11 (2019) 1252, https://doi.org/10.3390/polym11081252.

[10] A. Kayvani Fard, G. McKay, A. Buekenhoudt, H. Al Sulaiti, F. Motmans, M. Khraisheh, M. Atieh, Inorganic membranes: preparation and application for water treatment and desalination, Materials 11 (2018) 74, https://doi.org/10.3390/ma11010074.

[11] B. Hofs, J. Ogier, D. Vries, E.F. Beerendonk, E.R. Cornelissen, Comparison of ceramic and polymeric membrane permeability and fouling using surface water, Separ. Purif. Technol. 79 (2011) 365–374, https://doi.org/10.1016/j.seppur.2011.03.025.

[12] M. Padaki, R. Surya Murali, M.S. Abdullah, N. Misdan, A. Moslehyani, M. A. Kassim, N. Hilal, A.F. Ismail, Membrane technology enhancement in oil–water separation. A review, Desalination 357 (2015) 197–207, https://doi.org/10.1016/j.desal.2014.11.023.

[13] V. Gitis, G. Rothenberg, Ceramic Membranes: New Opportunities and Practical Applications, John Wiley & Sons, 2016.

[14] T. Tsuru, Inorganic porous membranes for liquid phase separation, Separ. Purif. Methods 30 (2001) 191–220, https://doi.org/10.1081/SPM-100108159.

[15] M. Chen, S.G.J. Heijman, L.C. Rietveld, State-of-the-art ceramic membranes for oily wastewater treatment: modification and application, Membranes 11 (2021), https://doi.org/10.3390/membranes11110888.

[16] H. Qi, G. Zhu, L. Li, N. Xu, Fabrication of a sol–gel derived microporous zirconia membrane for nanofiltration, J. Sol. Gel Sci. Technol. 62 (2012) 208–216, https://doi.org/10.1007/s10971-012-2711-0.

[17] C. Li, W. Sun, Z. Lu, X. Ao, S. Li, Ceramic nanocomposite membranes and membrane fouling: a review, Water Res. 175 (2020), 115674, https://doi.org/10.1016/j.watres.2020.115674.

[18] A. Basile, F. Gallucci, Membranes for Membrane Reactors: Preparation, Optimization and Selection, John Wiley & Sons, 2010.

[19] T. Van Gestel, D. Sebold, Hydrothermally stable mesoporous ZrO 2 membranes prepared by a facile nanoparticle deposition process, Separ. Purif. Technol. 221 (2019) 399–407, https://doi.org/10.1016/j.seppur.2019.03.066.

[20] T. Van Gestel, C. Vandecasteele, A. Buekenhoudt, C. Dotremont, J. Luyten, B. Van Der Bruggen, G. Maes, Corrosion properties of alumina and titania NF membranes, J. Membr. Sci. 214 (2003) 21–29, https://doi.org/10.1016/S0376-7388(02)00517-3.

[21] H. Verweij, Inorganic membranes, Curr. Opin. Chem. Eng. 1 (2012) 156–162, https://doi.org/10.1016/j.coche.2012.03.006.

[22] A. Buekenhoudt, Stability of porous ceramic membranes, in: Membr. Sci. Technol., 2008, pp. 1–31, https://doi.org/10.1016/S0927-5193(07)13001-1.

[23] A. Samadi, L. Gao, L. Kong, Y. Orooji, S. Zhao, Waste-derived low-cost ceramic membranes for water treatment: opportunities, challenges and future directions, Resour. Conserv. Recycl. 185 (2022), 106497, https://doi.org/10.1016/j.resconrec.2022.106497.

[24] W. Puthai, M. Kanezashi, H. Nagasawa, T. Tsuru, SiO2-ZrO2 nanofiltration membranes of different Si/Zr molar ratios: stability in hot water and acid/alkaline solutions, J. Membr. Sci. 524 (2017) 700–711, https://doi.org/10.1016/j.memsci.2016.11.045.

[25] L. Sun, Z. Wang, B. Gao, Ceramic membranes originated from cost effective and abundant natural minerals and industrial wastes for broad applications - a review, Desalin. WATER Treat. 201 (2020) 121–138, https://doi.org/10.5004/dwt.2020.25910.

[26] J. Caro, M. Noack, P. Kölsch, R. Schäfer, Zeolite membranes – state of their development and perspective, Microporous Mesoporous Mater. 38 (2000) 3–24, https://doi.org/10.1016/S1387-1811(99)00295-4.

[27] E. Eray, V.M. Candelario, V. Boffa, H. Safafar, D.N. Østedgaard-Munck, N. Zahrtmann, H. Kadrispahic, M.K. Jørgensen, A roadmap for the development and applications of silicon carbide membranes for liquid filtration: recent advancements, challenges, and perspectives, Chem. Eng. J. 414 (2021), 128826, https://doi.org/10.1016/j.cej.2021.128826.

[28] V. Boffa, E. Marino, Inorganic materials for upcoming water purification membranes, in: Curr. Trends Futur. Dev. Membr., Elsevier, 2020, pp. 117–140, https://doi.org/10.1016/B978-0-12-816823-3.00005-8.

[29] Y. Wang, Y. Liu, Z. Chen, Y. Liu, J. Guo, W. Zhang, P. Rao, G. Li, Recent progress in the pore size control of silicon carbide ceramic membranes, Ceram. Int. 48 (2022) 8960–8971, https://doi.org/10.1016/j.ceramint.2022.01.092.

[30] M.B. Asif, Z. Zhang, Ceramic membrane technology for water and wastewater treatment: a critical review of performance, full-scale applications, membrane fouling and prospects, Chem. Eng. J. 418 (2021), 129481, https://doi.org/10.1016/j.cej.2021.129481.

[31] X. Da, X. Chen, B. Sun, J. Wen, M. Qiu, Y. Fan, Preparation of zirconia nanofiltration membranes through an aqueous sol–gel process modified by glycerol for the treatment of wastewater with high salinity, J. Membr. Sci. 504 (2016) 29–39, https://doi.org/10.1016/j.memsci.2015.12.068.

[32] E. Eray, V. Boffa, M.K. Jørgensen, G. Magnacca, V.M. Candelario, Enhanced fabrication of silicon carbide membranes for wastewater treatment: from laboratory to industrial scale, J. Membr. Sci. (2020), 118080, https://doi.org/10.1016/j.memsci.2020.118080.

[33] M. Peron, S. Cogo, M. Bjelland, A. Bin Afif, A. Dadlani, E. Greggio, F. Berto, J. Torgersen, On the evaluation of ALD TiO2, ZrO2 and HfO2 coatings on corrosion and cytotoxicity performances, J. Magnes. Alloy. 9 (2021) 1806–1819, https://doi.org/10.1016/j.jma.2021.03.010.

[34] T. Van Gestel, H. Kruidhof, D.H.A. Blank, H.J.M. Bouwmeester, ZrO2 and TiO2 membranes for nanofiltration and pervaporationPart 1. Preparation and characterization of a corrosion-resistant ZrO2 nanofiltration membrane with a MWCO<300, J. Membr. Sci. 284 (2006) 128–136, https://doi.org/10.1016/j.memsci.2006.07.020.

[35] D. da Silva Biron, V. dos Santos, M. Zeni, Ceramic Membranes Applied in Separation Processes, 2018, https://doi.org/10.1007/978-3-319-58604-5.

[36] M.A. Rahman, M. Ha, D. Othman, A.F. Ismail, Morphological study of yttria-stabilized zirconia hollow fi bre membrane prepared using phase inversion/sintering technique, Ceram. Int. 41 (2015) 12543–12553, https://doi.org/10.1016/j.ceramint.2015.06.066.

[37] Y. Lu, T. Chen, X. Chen, M. Qiu, Y. Fan, Fabrication of TiO2-doped ZrO2 nanofiltration membranes by using a modified colloidal sol-gel process and its application in simulative radioactive effluent, J. Membr. Sci. 514 (2016) 476–486, https://doi.org/10.1016/j.memsci.2016.04.074.

[38] M. Qiu, X. Chen, Y. Fan, W. Xing, Ceramic membranes, in: Compr. Membr. Sci. Eng., Elsevier, 2017, pp. 270–297, https://doi.org/10.1016/B978-0-12-409547-2.12243-7.

[39] B. Düppenbecker, M. Engelhart, P. Cornel, Fouling mitigation in Anaerobic Membrane Bioreactor using fluidized glass beads: evaluation fitness for purpose of ceramic membranes, J. Membr. Sci. 537 (2017) 69–82, https://doi.org/10.1016/j.memsci.2017.05.018.

[40] S. Sun, H. Yao, W. Fu, L. Hua, G. Zhang, W. Zhang, Reactive Photo-Fenton ceramic membranes: synthesis, characterization and antifouling performance, Water Res. 144 (2018) 690–698, https://doi.org/10.1016/j.watres.2018.08.002.

[41] H. Qin, W. Guo, X. Huang, P. Gao, H. Xiao, Preparation of yttria-stabilized ZrO2 nanofiltration membrane by reverse micelles-mediated sol-gel process and its application in pesticide wastewater treatment, J. Eur. Ceram. Soc. 40 (2020) 145–154, https://doi.org/10.1016/j.jeurceramsoc.2019.09.023.

[42] D. Deemter, F.E.B. Coelho, I. Oller, S. Malato, A.M. Amat, Assessment of a novel photocatalytic TiO2-zirconia ultrafiltration membrane and combination with solar photo-fenton tertiary treatment of urban wastewater, Catalysts 12 (2022) 552, https://doi.org/10.3390/catal12050552.

[43] J.J. Porter, Recovery of polyvinyl alcohol and hot water from the textile wastewater using thermally stable membranes, J. Membr. Sci. 151 (1998) 45–53, https://doi.org/10.1016/S0376-7388(98)00236-1.

[44] H. Nagasawa, T. Omura, T. Asai, M. Kanezashi, T. Tsuru, Filtration of surfactant-stabilized oil-in-water emulsions with porous ceramic membranes: effects of membrane pore size and surface charge on fouling behavior, J. Membr. Sci. 610 (2020), 118210, https://doi.org/10.1016/j.memsci.2020.118210.

[45] K. Szymański, A.W. Morawski, S. Mozia, Effectiveness of treatment of secondary effluent from a municipal wastewater treatment plant in a photocatalytic membrane reactor and hybrid UV/H2O2 – ultrafiltration system, Chem. Eng. Process. - Process Intensif. 125 (2018) 318–324, https://doi.org/10.1016/j.cep.2017.11.015.

[46] B.D.P. Luogo, T. Salim, W. Zhang, N.B. Hartmann, F. Malpei, V.M. Candelario, Reuse of water in laundry applications with micro-and ultrafiltration ceramic membrane, Membranes 12 (2022) 1–11, https://doi.org/10.3390/membranes12020223.
[47] X. Da, J. Wen, Y. Lu, M. Qiu, Y. Fan, An aqueous sol-gel process for the fabrication of high-flux YSZ nanofiltration membranes as applied to the nanofiltration of dye wastewater, Separ. Purif. Technol. 152 (2015) 37–45, https://doi.org/10.1016/j.seppur.2015.07.050.
[48] T. Poerio, T. Denisi, R. Mazzei, F. Bazzarelli, E. Piacentini, L. Giorno, E. Curcio, Identification of fouling mechanisms in cross-flow microfiltration of olive-mills wastewater, J. Water Proc. Eng. 49 (2022), 103058, https://doi.org/10.1016/j.jwpe.2022.103058.
[49] P. Wang, X. Nanping, S. Jun, A pilot study of the treatment of waste rolling emulsion using zirconia microfiltration membranes, J. Membr. Sci. 173 (2000) 159–166, https://doi.org/10.1016/S0376-7388(00)00372-0.
[50] U. Aust, S. Benfer, M. Dietze, A. Rost, G. Tomandl, Development of microporous ceramic membranes in the system TiO2/ZrO2, J. Membr. Sci. 281 (2006) 463–471, https://doi.org/10.1016/j.memsci.2006.04.016.
[51] N. Gao, M. Li, W. Jing, Y. Fan, N. Xu, Improving the filtration performance of ZrO2 membrane in non-polar organic solvents by surface hydrophobic modification, J. Membr. Sci. 375 (2011) 276–283, https://doi.org/10.1016/j.memsci.2011.03.056.
[52] C. Guizard, A. Ayral, A. Julbe, Potentiality of organic solvents filtration with ceramic membranes. A comparison with polymer membranes, Desalination 147 (2002) 275–280, https://doi.org/10.1016/S0011-9164(02)00552-0.
[53] R. Iesako, T. Yoshioka, K. Nakagawa, T. Shintani, A. Matsuoka, E. Kamio, H. Matsuyama, Organic solvent permeation characteristics of TiO2-ZrO2 composite nanofiltration membranes prepared using organic chelating ligand to control pore size and surface property, Separ. Purif. Technol. 297 (2022), 121458, https://doi.org/10.1016/j.seppur.2022.121458.
[54] M. Boussemghoune, M. Chikhi, F. Balaska, Y. Ozay, N. Dizge, B. Kebabi, Preparation of a zirconia-based ceramic membrane and its application for drinking water treatment, Symmetry 12 (2020) 933, https://doi.org/10.3390/sym12060933.
[55] S. Kroll, C. Brandes, J. Wehling, L. Treccani, G. Grathwohl, K. Rezwan, Highly efficient enzyme-functionalized porous zirconia microtubes for bacteria filtration, Environ. Sci. Technol. 46 (2012) 8739–8747, https://doi.org/10.1021/es3006496.
[56] F.E. Bortot Coelho, D. Deemter, V.M. Candelario, V. Boffa, S. Malato, G. Magnacca, Development of a photocatalytic zirconia-titania ultrafiltration membrane with anti-fouling and self-cleaning properties, J. Environ. Chem. Eng. 9 (2021), 106671, https://doi.org/10.1016/j.jece.2021.106671.
[57] X. Zhang, L. Fan, F.A. Roddick, Influence of the characteristics of soluble algal organic matter released from Microcystis aeruginosa on the fouling of a ceramic microfiltration membrane, J. Membr. Sci. (2013) 23–29, https://doi.org/10.1016/j.memsci.2012.09.033, 425–426.
[58] M. Bodzek, K. Konieczny, Comparison of various membrane types and module configurations in the treatment of natural water by means of low-pressure membrane methods, Separ. Purif. Technol. 14 (1998) 69–78, https://doi.org/10.1016/S1383-5866(98)00061-6.
[59] J. Werner, B. Besser, C. Brandes, S. Kroll, K. Rezwan, Production of ceramic membranes with different pore sizes for virus retention, J. Water Proc. Eng. 4 (2014) 201–211, https://doi.org/10.1016/j.jwpe.2014.10.007.
[60] Y. Chung, Y.-M. Yun, Y.-J. Kim, Y.S. Hwang, S. Kang, Preparation of alumina-zirconia (Al-Zr) ceramic nanofiltration (NF) membrane for the removal of uranium in aquatic system, Water Supply 19 (2019) 789–795, https://doi.org/10.2166/ws.2018.123.
[61] S.A. An, J. Lee, J. Sim, C.G. Park, J.S. Lee, H. Rho, K.D. Park, H.S. Kim, Y.C. Woo, Evaluation of the advanced oxidation process integrated with microfiltration for reverse osmosis to treat semiconductor wastewater, Process Saf. Environ. Protect. 162 (2022) 1057–1066, https://doi.org/10.1016/j.psep.2022.05.010.
[62] T. Tsuru, H. Takezoe, M. Asaeda, Ion separation by porous silica-zirconia nanofiltration membranes, AIChE J. 44 (1998) 765–768, https://doi.org/10.1002/aic.690440324.
[63] A. Islam, B. Praveen Chakkravarthy Raghupathy, M.V. Sivakumaran, A. Kumar Keshri, Ceramic membrane for water filtration: addressing the various concerns at once, Chem. Eng. J. 446 (2022), 137386, https://doi.org/10.1016/j.cej.2022.137386.
[64] S. Cerneaux, I. Strużyńska, W.M. Kujawski, M. Persin, A. Larbot, Comparison of various membrane distillation methods for desalination using hydrophobic ceramic membranes, J. Membr. Sci. 337 (2009) 55–60, https://doi.org/10.1016/j.memsci.2009.03.025.
[65] A. Larbot, L. Gazagnes, S. Krajewski, M. Bukowska, Wojciech Kujawski, Water desalination using ceramic membrane distillation, Desalination 168 (2004) 367–372, https://doi.org/10.1016/j.desal.2004.07.021.
[66] R. Kreiter, M.D.A. Rietkerk, B.C. Bonekamp, H.M. van Veen, V.G. Kessler, J. F. Vente, Sol–gel routes for microporous zirconia and titania membranes, J. Sol. Gel Sci. Technol. 48 (2008) 203–211, https://doi.org/10.1007/s10971-008-1760-x.
[67] T. Fukumoto, T. Yoshioka, H. Nagasawa, M. Kanezashi, T. Tsuru, Development and gas permeation properties of microporous amorphous TiO2–ZrO2–organic composite membranes using chelating ligands, J. Membr. Sci. 461 (2014) 96–105, https://doi.org/10.1016/j.memsci.2014.02.031.
[68] R.S. Faibish, Y. Cohen, Fouling and rejection behavior of ceramic and polymer-modified ceramic membranes for ultrafiltration of oil-in-water emulsions and microemulsions, Colloids Surfaces A Physicochem. Eng. Asp. 191 (2001) 27–40, https://doi.org/10.1016/S0927-7757(01)00761-0.
[69] X. Wang, K. Sun, G. Zhang, F. Yang, S. Lin, Y. Dong, Robust zirconia ceramic membrane with exceptional performance for purifying nano-emulsion oily wastewater, Water Res. 208 (2022), 117859, https://doi.org/10.1016/j.watres.2021.117859.
[70] J.E. Zhou, Q. Chang, Y. Wang, J. Wang, G. Meng, Separation of stable oil-water emulsion by the hydrophilic nano-sized ZrO2 modified Al2O3 microfiltration membrane, Separ. Purif. Technol. 75 (2010) 243–248, https://doi.org/10.1016/j.seppur.2010.08.008.
[71] C. Yang, G. Zhang, N. Xu, J. Shi, Preparation and application in oil–water separation of ZrO2/α-Al2O3 MF membrane, J. Membr. Sci. 142 (1998) 235–243, https://doi.org/10.1016/S0376-7388(97)00336-0.
[72] X. Zhang, J. Hu, Q. Chang, Y. Wang, J. Zhou, T. Zhao, Y. Jiang, X. Liu, Influences of internal coagulant composition on microstructure and properties of porous YSZ hollow fibre membranes for water treatment, Separ. Purif. Technol. 147 (2015) 337–345, https://doi.org/10.1016/j.seppur.2015.01.027.
[73] F.E. Bortot Coelho, N.N. Kaiser, G. Magnacca, V.M. Candelario, Corrosion resistant ZrO2/SiC ultrafiltration membranes for wastewater treatment and operation in harsh environments, J. Eur. Ceram. Soc. 41 (2021) 7792–7806, https://doi.org/10.1016/j.jeurceramsoc.2021.07.054.
[74] J. Cakl, I. Bauer, P. Doleček, P. Mikulášek, Effects of backflushing conditions on permeate flux in membrane crossflow microfiltration of oil emulsion, Desalination 127 (2000) 189–198, https://doi.org/10.1016/S0011-9164(99)00204-0.
[75] A. Murić, I. Petrinić, M.L. Christensen, Comparison of ceramic and polymeric ultrafiltration membranes for treating wastewater from metalworking industry, Chem. Eng. J. 255 (2014) 403–410, https://doi.org/10.1016/j.cej.2014.06.009.
[76] Y. Huang, H. Liu, Y. Wang, G. Song, L. Zhang, Industrial application of ceramic ultrafiltration membrane in cold-rolling emulsion wastewater treatment, Separ. Purif. Technol. 289 (2022), 120724, https://doi.org/10.1016/j.seppur.2022.120724.
[77] M.Đ. Carić, S.D. Milanović, D.M. Krstić, M.N. Tekić, Fouling of inorganic membranes by adsorption of whey proteins, J. Membr. Sci. 165 (2000) 83–88, https://doi.org/10.1016/S0376-7388(99)00221-5.
[78] W. Doyen, W. Adriansens, B. Molenberghs, R. Leysen, A comparison between polysulfone, zirconia and organo-mineral membranes for use in ultrafiltration, J. Membr. Sci. 113 (1996) 247–258, https://doi.org/10.1016/0376-7388(95)00124-7.
[79] M. Sterner, F. Gröndahl, Extraction of laminarin from Saccharina latissima seaweed using cross-flow filtration, J. Appl. Phycol. 33 (2021) 1825–1844, https://doi.org/10.1007/s10811-021-02398-z.
[80] Y. Chen, M. Rovira-Bru, F. Giralt, Y. Cohen, Hydraulic resistance and protein fouling resistance of a zirconia membrane with a tethered PVP layer, Water 13 (2021) 951, https://doi.org/10.3390/w13070951.
[81] S. Dumon, H. Barnier, Ultrafiltration of protein solutions on ZrO2 membranes. The influence of surface chemistry and solution chemistry on adsorption, J. Membr. Sci. 74 (1992) 289–302, https://doi.org/10.1016/0376-7388(92)80068-U.
[82] M. Li, Y. Zhao, S. Zhou, W. Xing, F.-S. Wong, Resistance analysis for ceramic membrane microfiltration of raw soy sauce, J. Membr. Sci. 299 (2007) 122–129, https://doi.org/10.1016/j.memsci.2007.04.033.
[83] S. Zhou, A. Xue, Y. Zhang, M. Li, J. Wang, Y. Zhao, W. Xing, Fabrication of temperature-responsive ZrO2 tubular membranes, grafted with poly (N-isopropylacrylamide) brush chains, for protein removal and easy cleaning, J. Membr. Sci. 450 (2014) 351–361, https://doi.org/10.1016/j.memsci.2013.09.011.
[84] J. Wen, C. Yang, X. Chen, M. Qiu, Y. Fan, Effective and efficient fabrication of high-flux tight ZrO2 ultrafiltration membranes using a nanocrystalline precursor, J. Membr. Sci. 634 (2021), 119378, https://doi.org/10.1016/j.memsci.2021.119378.
[85] J. Randon, P. Blanc, R. Paterson, Modification of ceramic membrane surfaces using phosphoric acid and alkyl phosphonic acids and its effects on ultrafiltration of BSA protein, J. Membr. Sci. 98 (1995) 119–129, https://doi.org/10.1016/0376-7388(94)00183-Y.
[86] S. Schiffer, A. Matyssek, M. Hartinger, P. Bolduan, P. Mund, U. Kulozik, Effects of selective layer properties of ceramic multi-channel microfiltration membranes on the milk protein fractionation, Separ. Purif. Technol. 259 (2021), 118050, https://doi.org/10.1016/j.seppur.2020.118050.
[87] M. Kumar, G. Pugazhenthi, D. Vasanth, Synthesis of zirconia-ceramic composite membrane employing a low-cost precursor and evaluation its performance for separation of microbially produced silver nanoparticles, J. Environ. Chem. Eng. 10 (2022), 107569, https://doi.org/10.1016/j.jece.2022.107569.
[88] T. Van Gestel, D. Sebold, H. Kruidhof, H.J.M. Bouwmeester, ZrO2 and TiO2 membranes for nanofiltration and pervaporation. Part 2. Development of ZrO2 and TiO2 toplayers for pervaporation, J. Membr. Sci. 318 (2008) 413–421, https://doi.org/10.1016/j.memsci.2008.03.003.
[89] A.F. Ismail, D. Rana, T. Matsuura, H.C. Foley, Carbon-based Membranes for Separation Processes, Springer New York, New York, NY, 2011, https://doi.org/10.1007/978-0-387-78991-0.
[90] A. Innovations, Membranes - atech innovations GmbH (n.d.), https://www.atech-innovations.com/en/products/membranes. (Accessed 23 November 2022).
[91] A. Group, KLEANSEP ultrafiltration system for degreasing baths | alsys (n.d.), https://www.alsys-group.com/en/membrane-en/kleansep-ultrafiltration-system-for-degreasing-baths/. (Accessed 23 November 2022).

[92] Novasep, Kerasep® mineral membranes for industrial cross-flow filtration, Novasep, (n.d.), https://www.novasep.com/process-solutions/fermentation-and-bio-based/products/kerasep-mineral-membranes-for-industrial-cross-flow-filtration.html. (Accessed 23 November 2022).
[93] Inopor GmbH, Membranes - Inopor – the Cutting Edge of Nano-Filtration, 2017. https://www.inopor.com/en/products/membranes.html. (Accessed 23 November 2022).
[94] T. Industries, tami industries: INSIDE CéRAM™ (n.d.), https://www.tami-industries.com/en/produits/inside-ceram-4/. (Accessed 23 November 2022).
[95] C. Pall, Membralox® Ceramic Membranes and Modules, 2007. https://shop.pall.com/us/en/products/ceramic-filters/zidgri78m7m?CategoryName=ceramic-filters&CatalogID=products&tracking=searchterm:Membralox. (Accessed 23 November 2022).
[96] S. Amin, D. Rashad, M. Mansour, H. Abdallah, A systematic literature review of ceramic membranes applications in water treatment, Egypt, J. Chem. 65 (2021), https://doi.org/10.21608/ejchem.2021.105802.4871, 0–0.
[97] S.M. Samaei, S. Gato-Trinidad, A. Altaee, The application of pressure-driven ceramic membrane technology for the treatment of industrial wastewaters – a review, Separ. Purif. Technol. 200 (2018) 198–220, https://doi.org/10.1016/j.seppur.2018.02.041.
[98] C. Mazzoni, F. Orlandini, S. Bandini, Role of electrolyte type on TiO2–ZrO2 nanofiltration membranes performances, Desalination 240 (2009) 227–235, https://doi.org/10.1016/j.desal.2007.11.074.
[99] S. Bouhallab, G. Henry, Transmission of a hydrophobic peptide through an inorganic ultrafiltration membrane: effect of membrane support, J. Membr. Sci. 104 (1995) 73–79, https://doi.org/10.1016/0376-7388(95)00013-3.
[100] J. Fan, H. Ohya, T. Suga, H. Ohashi, K. Yamashita, S. Tsuchiya, M. Aihara, T. Takeuchi, Y. Negishi, High flux zirconia composite membrane for hydrogen separation at elevated temperature, J. Membr. Sci. 170 (2000) 113–125, https://doi.org/10.1016/S0376-7388(99)00363-4.
[101] M. Asaeda, Y. Sakou, J. Yang, K. Shimasaki, Stability and performance of porous silica–zirconia composite membranes for pervaporation of aqueous organic solutions, J. Membr. Sci. 209 (2002) 163–175, https://doi.org/10.1016/S0376-7388(02)00327-7.
[102] T. Tsuru, T. Sudoh, T. Yoshioka, M. Asaeda, Nanofiltration in non-aqueous solutions by porous silica–zirconia membranes, J. Membr. Sci. 185 (2001) 253–261, https://doi.org/10.1016/S0376-7388(00)00651-7.
[103] F. Shojai, T.A. Mäntylä, Chemical stability of yttria doped zirconia membranes in acid and basic aqueous solutions: chemical properties, effect of annealing and ageing time, Ceram. Int. 27 (2001) 299–307, https://doi.org/10.1016/S0272-8842(00)00080-8.
[104] A. Larbot, J.-P. Fabre, C. Guizard, L. Cot, J. Gillot, New inorganic ultrafiltration membranes: titania and zirconia membranes, J. Am. Ceram. Soc. 72 (1989) 257–261, https://doi.org/10.1111/j.1151-2916.1989.tb06111.x.
[105] A.F.M. Leenaars, K. Keizer, A.J. Burggraaf, The preparation and characterization of alumina membranes with ultra-fine pores, J. Mater. Sci. 19 (1984) 1077–1088, https://doi.org/10.1007/BF01120016.
[106] S. Li, C. Wei, L. Zhou, P. Wang, Q. Meng, Z. Xie, Sol-gel derived zirconia membrane on silicon carbide substrate, J. Eur. Ceram. Soc. (2019), https://doi.org/10.1016/j.jeurceramsoc.2019.04.054, 0–1.
[107] J. Etienne, A. Larbot, A. Julbe, C. Guizard, L. Cot, A microporous zirconia membrane prepared by the sol-gel process from zirconyl oxalate, J. Membr. Sci. 86 (1994) 95–102, https://doi.org/10.1016/0376-7388(93)E0141-6.
[108] G. Zhu, Q. Jiang, H. Qi, N. Xu, Effect of sol size on nanofiltration performance of a sol-gel derived microporous zirconia membrane, Chin. J. Chem. Eng. 23 (2015) 31–41, https://doi.org/10.1016/j.cjche.2014.09.045.
[109] H. Qin, W. Guo, P. Gao, H. Xiao, Customization of ZrO2 loose/tight bilayer ultrafiltration membranes by reverse micelles-mediated aqueous sol-gel process for wastewater treatment, J. Eur. Ceram. Soc. 41 (2021) 2724–2733, https://doi.org/10.1016/j.jeurceramsoc.2020.11.008.
[110] S. Benfer, U. Popp, H. Richter, C. Siewert, G. Tomandl, Development and characterization of ceramic nanofiltration membranes, Separ. Purif. Technol. 22–23 (2001) 231–237, https://doi.org/10.1016/S1383-5866(00)00133-7.
[111] X. Da, D. Zou, X. Chen, M. Qiu, W. Ke, Y. Fan, Influence of compatibility between sol and intermediate layer on the performance of yttria-stabilized zirconia nanofiltration membrane, Ceram. Int. 47 (2021) 22801–22809, https://doi.org/10.1016/j.ceramint.2021.04.299.
[112] T. Okubo, T. Takahashi, M. Sadakata, H. Nagamoto, Crack-free porous YSZ membrane via controlled synthesis of zirconia sol, J. Membr. Sci. 118 (1996) 151–157, https://doi.org/10.1016/0376-7388(96)00085-3.
[113] R. Vacassy, C. Guizard, V. Thoraval, L. Cot, Synthesis and characterization of microporous zirconia powders: application in nanofilters and nanofiltration characteristics, J. Membr. Sci. 132 (1997) 109–118, https://doi.org/10.1016/S0376-7388(97)00051-3.
[114] S. Li, C. Wei, P. Wang, P. Gao, L. Zhou, G. Wen, Zirconia ultrafiltration membranes on silicon carbide substrate: microstructure and water flux, J. Eur. Ceram. Soc. 40 (2020) 4290–4298, https://doi.org/10.1016/j.jeurceramsoc.2020.04.020.
[115] S.O. Lawal, H. Nagasawa, T. Tsuru, M. Kanezashi, Enhancement of the H2-permselectivity of a silica-zirconia composite membrane enabled by ligand-ceramic to carbon-ceramic transformation, J. Membr. Sci. 642 (2022), 119948, https://doi.org/10.1016/j.memsci.2021.119948.
[116] H. Guo, S. Zhao, X. Wu, H. Qi, Fabrication and characterization of TiO2/ZrO2 ceramic membranes for nanofiltration, Microporous Mesoporous Mater. 260 (2018) 125–131, https://doi.org/10.1016/j.micromeso.2016.03.011.
[117] Y. Zhang, X. Shan, Z. Jin, Y. Wang, Synthesis of sulfated Y-doped zirconia particles and effect on properties of polysulfone membranes for treatment of wastewater containing oil, J. Hazard Mater. 192 (2011) 559–567, https://doi.org/10.1016/j.jhazmat.2011.05.058.
[118] N.N. Mohammad Jafri, J. Jaafar, M.H. Dzarfan Othman, M.A. Rahman, F. Aziz, N. Yusof, W.N. Wan Salleh, A. Fauzi Ismail, Titanium dioxide hollow nanofibers for enhanced photocatalytic activities, Mater. Today Proc. 46 (2021) 2004–2011, https://doi.org/10.1016/j.matpr.2021.02.662.
[119] A. Bouazizi, M. Breida, B. Achiou, M. Ouammou, J.I. Calvo, A. Aaddane, S. A. Younssi, Removal of dyes by a new nano–TiO 2 ultrafiltration membrane deposited on low-cost support prepared from natural Moroccan bentonite, Appl. Clay Sci. 149 (2017) 127–135, https://doi.org/10.1016/j.clay.2017.08.019.
[120] X. Ding, Y. Fan, N. Xu, A new route for the fabrication of TiO2 ultrafiltration membranes with suspension derived from a wet chemical synthesis, J. Membr. Sci. 270 (2006) 179–186, https://doi.org/10.1016/j.memsci.2005.07.003.
[121] X. Zhang, D.K. Wang, J.C. Diniz Da Costa, Recent progresses on fabrication of photocatalytic membranes for water treatment, Catal. Today 230 (2014) 47–54, https://doi.org/10.1016/j.cattod.2013.11.019.
[122] S. Leong, A. Razmjou, K. Wang, K. Hapgood, X. Zhang, H. Wang, TiO2based photocatalytic membranes: a review, J. Membr. Sci. 472 (2014) 167–184, https://doi.org/10.1016/j.memsci.2014.08.016.
[123] M. Qiu, Y. Fan, N. Xu, Preparation of supported zirconia ultrafiltration membranes with the aid of polymeric additives, J. Membr. Sci. 348 (2010) 252–259, https://doi.org/10.1016/j.memsci.2009.11.009.
[124] A. Lee, J.W. Elam, S.B. Darling, Membrane materials for water purification: design, development, and application, Environ. Sci. Water Res. Technol. 2 (2016) 17–42, https://doi.org/10.1039/c5ew00159e.
[125] J.M.S. Henis, M.K. Tripodi, Composite hollow fiber membranes for gas separation: the resistance model approach, J. Membr. Sci. 8 (1981) 233–246, https://doi.org/10.1016/S0376-7388(00)82312-1.
[126] B.C. Bonekamp, Preparation of asymmetric ceramic membrane supports by dip-coating, in: A.J. Burggraaf, L.B.T. M.S, T. Cot (Eds.), Fundam. Inorg. Membr. Sci. Technol., Elsevier, 1996, pp. 141–225, https://doi.org/10.1016/S0927-5193(96)80009-X.
[127] C. Guizard, A. Ayral, M. Barboiu, A. Julbe, Sol–gel processed membranes, in: L. Klein, M. Aparicio, A. Jitianu (Eds.), Handb. Sol-Gel Sci. Technol., Springer International Publishing, Cham, 2016, pp. 1–47, https://doi.org/10.1007/978-3-319-19454-7_58-1.
[128] Scopus/Elsevier, Scopus Search, 2022. https://www.scopus.com/search/. (Accessed 20 May 2022).
[129] M.V. Landau, Sol-gel process, in: Handb. Heterog. Catal., Wiley-VCH Verlag GmbH & Co. KGaA, Weinheim, Germany, 2008, https://doi.org/10.1002/9783527610044.hetcat0009.
[130] A. Taavoni-Gilan, E. Taheri-Nassaj, M. Shamsipur, Synthesis of nanostructured titania/zirconia membrane and investigation of its physical separation and photocatalytic properties in treatment of textile industries wastewater, J. Iran. Chem. Soc. 15 (2018) 2759–2769, https://doi.org/10.1007/s13738-018-1463-3.
[131] J.C.S. Wu, L.C. Cheng, An improved synthesis of ultrafiltration zirconia membranes via the sol- gel route using alkoxide precursor, J. Membr. Sci. 167 (2000) 253–261, https://doi.org/10.1016/S0376-7388(99)00294-X.
[132] R. Nielsen, Zirconium and zirconium compounds, in: Ullmann's Encycl. Ind. Chem., Wiley-VCH Verlag GmbH & Co. KGaA, Weinheim, Germany, 2000, https://doi.org/10.1002/14356007.a28_543.
[133] İ. Erdem, Sol-gel Applications for Ceramic Membrane Preparation, AIP Conf. Proc., 2017, 020011, https://doi.org/10.1063/1.4975426.
[134] O.P. Linnik, Synthesis and characterization of nitrogen and zirconium ions doped TiO2 films for photocatalytic application, Him. Fiz. Ta Tehnol. Poverhni. 7 (2016) 453–462, https://doi.org/10.15407/hftp07.04.453.
[135] S. Anisah, W. Puthai, M. Kanezashi, H. Nagasawa, T. Tsuru, Preparation, characterization, and evaluation of TiO2-ZrO2 nanofiltration membranes fired at different temperatures, J. Membr. Sci. 564 (2018) 691–699, https://doi.org/10.1016/j.memsci.2018.07.072.
[136] S. Rossignol, F. Gérard, D. Duprez, Effect of the preparation method on the properties of zirconia-ceria materials, J. Mater. Chem. 9 (1999) 1615–1620, https://doi.org/10.1039/a900536f.
[137] B.M. Novak, Hybrid Nanocomposite Materials?between inorganic glasses and organic polymers, Adv. Mater. 5 (1993) 422–433, https://doi.org/10.1002/adma.19930050603.
[138] S.H. Shah, R. Mirza, T.A. Butt, M. Bilal, M.S.A. Yasser, A. Ali, M.A. Ali, A. Baig, R. Z. Shah, M.H. Shah, B.A.Z. Amin, M.H.H. Bin Asad, M. Saqib, A.J. Shaikh, Nanoporous zirconia membranes for separation of hydrogen from carbon dioxide, Pol. J. Environ. Stud. 30 (2021) 2313–2323, https://doi.org/10.15244/pjoes/127385.
[139] C.C. Coterillo, T. Yokoo, T. Yoshioka, T. Tsuru, M. Asaeda, Synthesis and characterization of microporous ZrO2 membranes for gas permeation at 200°c, Separ. Sci. Technol. 46 (2011) 1224–1230, https://doi.org/10.1080/01496395.2011.556098.
[140] Y.S. Lin, C.H. Chang, R. Gopalan, Improvement of thermal stability of porous nanostructured ceramic membranes, Ind. Eng. Chem. Res. 33 (1994) 860–870, https://doi.org/10.1021/ie00028a012.
[141] R.R. Bhave, Inorganic Membranes Synthesis, Characteristics and Applications, Springer Netherlands, Dordrecht, 1991, https://doi.org/10.1007/978-94-011-6547-1.
[142] I. Dobrosz-Gómez, I. Kocemba, J.M. Rynkowski, Au/Ce1−xZrxO2 as effective catalysts for low-temperature CO oxidation, Appl. Catal. B Environ. 83 (2008) 240–255, https://doi.org/10.1016/j.apcatb.2008.02.012.

[143] I. John Berlin, L.V. Maneeshya, J.K. Thomas, P.V. Thomas, K. Joy, Enhancement of photoluminescence emission intensity of zirconia thin films via aluminum doping for the application of solid state lighting in light emitting diode, J. Lumin. 132 (2012) 3077–3081, https://doi.org/10.1016/j.jlumin.2012.06.027.
[144] Y.L. Soo, P.J. Chen, S.H. Huang, T.J. Shiu, T.Y. Tsai, Y.H. Chow, Y.C. Lin, S. C. Weng, S.L. Chang, G. Wang, C.L. Cheung, R.F. Sabirianov, W.N. Mei, F. Namavar, H. Haider, K.L. Garvin, J.F. Lee, H.Y. Lee, P.P. Chu, Local structures surrounding Zr in nanostructurally stabilized cubic zirconia: structural origin of phase stability, J. Appl. Phys. 104 (2008), https://doi.org/10.1063/1.3041490.
[145] C. Ricca, A. Ringuedé, M. Cassir, C. Adamo, F. Labat, A comprehensive DFT investigation of bulk and low-index surfaces of ZrO2 polymorphs, J. Comput. Chem. 36 (2015) 9–21, https://doi.org/10.1002/jcc.23761.
[146] Y. Zhang, H.X. Chen, L. Duan, J. Bin Fan, L. Ni, V. Ji, A comparison study of the structural and mechanical properties of cubic, tetragonal, monoclinic, and three orthorhombic phases of ZrO2, J. Alloys Compd. 749 (2018) 283–292, https://doi.org/10.1016/j.jallcom.2018.03.253.
[147] H.G. Scott, Phase relationships in the zirconia-yttria system, J. Mater. Sci. 10 (1975) 1527–1535, https://doi.org/10.1007/BF01031853.
[148] M. Yashima, M. Kakihana, M. Yoshimura, Metastable-stable phase diagrams in the zirconia-containing systems utilized in solid-oxide fuel cell application, Solid State Ionics 86–88 (1996) 1131–1149, https://doi.org/10.1016/0167-2738(96)00386-4.
[149] G. Witz, V. Shklover, W. Steurer, S. Bachegowda, H.P. Bossmann, Phase evolution in yttria-stabilized zirconia thermal barrier coatings studied by rietveld refinement of X-ray powder diffraction patterns, J. Am. Ceram. Soc. 90 (2007) 2935–2940, https://doi.org/10.1111/j.1551-2916.2007.01785.x.
[150] L. Fei, L. Yanhuai, S. Zhongxiao, X. Kewei, M. Dayan, G. Bo, C. Hong, Grain growth characteristics of hydrothermally prepared yttria stabilized zirconia nanocrystals during calcination, Rare Met. Mater. Eng. 46 (2017) 899–905, https://doi.org/10.1016/S1875-5372(17)30119-4.
[151] B. Song, E. Ruiz-Trejo, N.P. Brandon, Enhanced mechanical stability of Ni-YSZ scaffold demonstrated by nanoindentation and Electrochemical Impedance Spectroscopy, J. Power Sources 395 (2018) 205–211, https://doi.org/10.1016/j.jpowsour.2018.05.075.
[152] T. Götsch, W. Wallisch, M. Stöger-Pollach, B. Klötzer, S. Penner, From zirconia to yttria: sampling the YSZ phase diagram using sputter-deposited thin films, AIP Adv. 6 (2016), https://doi.org/10.1063/1.4942818.
[153] S.Y. Gómez, A.L. da Silva, D. Gouvêa, R.H.R. Castro, D. Hotza, Nanocrystalline yttria-doped zirconia sintered by fast firing, Mater. Lett. 166 (2016) 196–200, https://doi.org/10.1016/j.matlet.2015.12.042.
[154] B.C. Bonekamp, R. Kreiter, J.F. Vente, Sol-Gel Approaches in the Synthesis of Membrane Materials for Nanofiltration and Pervaporation, 2008, pp. 47–65, https://doi.org/10.1007/978-1-4020-8514-7_3.
[155] A.C. Pierre, Introduction to Sol-Gel Processing, Springer US, Boston, MA, 1998, https://doi.org/10.1007/978-1-4615-5659-6.
[156] Y. Gu, K. Kusakabe, S. Morooka, Effect of chelating agent 1,5-diaminopentane on the microstructures of sol-gel derived zirconia membranes, Separ. Sci. Technol. 36 (2001) 3689–3700, https://doi.org/10.1081/SS-100108356.
[157] J. Etienne, A. Larbot, C. Guizard, L. Cot, J.A. Alary, Preparation and characterization of a zirconyl oxalate gel, J. Non-Cryst. Solids 125 (1990) 224–229, https://doi.org/10.1016/0022-3093(90)90852-D.
[158] Q. Xu, M.A. Anderson, Sol–gel route to synthesis of microporous ceramic membranes: preparation and characterization of microporous TiO2 and ZrO2 xerogels, J. Am. Ceram. Soc. 77 (1994) 1939–1945, https://doi.org/10.1111/j.1151-2916.1994.tb07074.x.
[159] Y. Cai, Y. Wang, X. Chen, M. Qiu, Y. Fan, Modified colloidal sol-gel process for fabrication of titania nanofiltration membranes with organic additives, J. Membr. Sci. 476 (2015) 432–441, https://doi.org/10.1016/j.memsci.2014.11.034.
[160] X. Ju, P. Huang, N. Xu, J. Shi, Influences of sol and phase stability on the structure and performance of mesoporous zirconia membranes, J. Membr. Sci. 166 (2000) 41–50, https://doi.org/10.1016/S0376-7388(99)00243-4.
[161] T. Tsuru, S.I. Wada, S. Izumi, M. Asaeda, Silica-zirconia membranes for nanofiltration, J. Membr. Sci. 149 (1998) 127–135, https://doi.org/10.1016/S0376-7388(98)00163-X.
[162] S. Lawal, M. Kanezashi, H. Nagasawa, T. Tsuru, Development of an acetylacetonate-modified silica-zirconia composite membrane applicable to gas separation, J. Membr. Sci. 599 (2020), 117844, https://doi.org/10.1016/j.memsci.2020.117844.
[163] W. Puthai, M. Kanezashi, H. Nagasawa, K. Wakamura, H. Ohnishi, T. Tsuru, Effect of firing temperature on the water permeability of SiO2–ZrO2 membranes for nanofiltration, J. Membr. Sci. 497 (2016) 348–356, https://doi.org/10.1016/j.memsci.2015.09.040.
[164] G. Oskam, A. Nellore, R.L. Penn, P.C. Searson, The growth kinetics of TiO 2 nanoparticles from titanium(IV) alkoxide at high water/titanium ratio, J. Phys. Chem. B 107 (2003) 1734–1738, https://doi.org/10.1021/jp021237f.
[165] B.E. Yoldas, Zirconium oxides formed by hydrolytic condensation of alkoxides and parameters that affect their morphology, J. Mater. Sci. 21 (1986) 1080–1086, https://doi.org/10.1007/BF01117398.
[166] B. Yoldas, Alumina sol preparation from alkoxides, AMER. CERAM. SOC. BULL. 54 (1975).
[167] K.B. Singh, M.S. Tirumkudulu, Cracking in drying colloidal films, Phys. Rev. Lett. 98 (2007), 218302, https://doi.org/10.1103/PhysRevLett.98.218302.
[168] M.S. Tirumkudulu, W.B. Russel, Cracking in drying latex films, Langmuir 21 (2005) 4938–4948, https://doi.org/10.1021/la048298k.
[169] V.G. Kessler, G.I. Spijksma, G.A. Seisenbaeva, S. Håkansson, D.H.A. Blank, H.J. M. Bouwmeester, New insight in the role of modifying ligands in the sol-gel processing of metal alkoxide precursors: a possibility to approach new classes of materials, J. Sol. Gel Sci. Technol. 40 (2006) 163–179, https://doi.org/10.1007/s10971-006-9209-6.
[170] J. Sekulić, A. Magraso, J.E. ten Elshof, D.H.A. Blank, Influence of ZrO2 addition on microstructure and liquid permeability of mesoporous TiO2 membranes, Microporous Mesoporous Mater. 72 (2004) 49–57, https://doi.org/10.1016/j.micromeso.2004.04.017.
[171] G.I. Spijksma, C. Huiskes, N.E. Benes, H. Kruidhof, D.H.A. Blank, V.G. Kessler, H. J.M. Bouwmeester, Microporous Zirconia-Titania composite membranes derived from diethanolamine-modified precursors, Adv. Mater. 18 (2006) 2165–2168, https://doi.org/10.1002/adma.200502568.
[172] P. Boch, J.-C. Niepce, Ceramic Materials: Processes, Properties, and Applications, John Wiley & Sons, 2010.
[173] S.K. Amin, H.A.M. Abdallah, M.H. Roushdy, S.A. El-Sherbiny, An overview of production and development of ceramic membranes, Int. J. Appl. Eng. Res. 11 (2016) 7708–7721.
[174] M.R. O, H. Mukhtar, Review on development of ceramic membrane from sol-gel route: parameters affecting characteristics of the membrane, IIUM Eng. J. 1 (2000) 1–6, https://doi.org/10.31436/iiumej.v1i2.334.
[175] J. Kim, Y.S. Lin, Sol-gel synthesis and characterization of yttria stabilized zirconia membranes, J. Membr. Sci. 139 (1998) 75–83, https://doi.org/10.1016/S0376-7388(97)00250-0.
[176] Q. Xu, M.A. Anderson, Sol-gel route to synthesis of microporous ceramic membranes: thermal stability of TiO2-ZrO2Mixed oxides, J. Am. Ceram. Soc. 76 (1993) 2093–2097, https://doi.org/10.1111/j.1151-2916.1993.tb08338.x.
[177] İ. Erdem, M. Çiftçioğlu, Modification of surface charge characteristics for unsupported nanostructured titania–zirconia UF/NF membrane top layers with calcination temperature, J. Australas. Ceram. Soc. 56 (2020) 203–215, https://doi.org/10.1007/s41779-019-00352-4.
[178] R. Nisticò, D. Scalarone, G. Magnacca, Sol-gel chemistry, templating and spin-coating deposition: a combined approach to control in a simple way the porosity of inorganic thin films/coatings, Microporous Mesoporous Mater. 248 (2017) 18–29, https://doi.org/10.1016/j.micromeso.2017.04.017.
[179] A. Darmawan, L. Karlina, I. Khairunnisak, R.E. Saputra, C. Azmiyawati, Y. Astuti, A.P. Noorita, Hydrophobic silica thin film derived from dimethyldimethoxysilane-tetraethylorthosilicate for desalination, Thin Solid Films 734 (2021), 138865, https://doi.org/10.1016/j.tsf.2021.138865.
[180] W. Puthai, M. Kanezashi, H. Nagasawa, T. Tsuru, Nanofiltration performance of SiO2-ZrO2 membranes in aqueous solutions at high temperatures, Separ. Purif. Technol. 168 (2016) 238–247, https://doi.org/10.1016/j.seppur.2016.05.028.
[181] T. Tsuru, M. Miyawaki, T. Yoshioka, M. Asaeda, Reverse osmosis of nonaqueous solutions through porous silica-zirconia membranes, AIChE J. 52 (2006) 522–531, https://doi.org/10.1002/aic.10654.
[182] T. Van Gestel, D. Sebold, W.A. Meulenberg, M. Bram, H.P. Buchkremer, Manufacturing of new nano-structured ceramic-metallic composite microporous membranes consisting of ZrO2, Al2O3, TiO2 and stainless steel, Solid State Ionics 179 (2008) 1360–1366, https://doi.org/10.1016/j.ssi.2008.02.046.
[183] S. Anisah, M. Kanezashi, H. Nagasawa, T. Tsuru, Hydrothermal stability and permeation properties of TiO2-ZrO2 (5/5) nanofiltration membranes at high temperatures, Separ. Purif. Technol. 212 (2019) 1001–1012, https://doi.org/10.1016/j.seppur.2018.12.006.
[184] G.N. Shao, S.M. Imran, S.J. Jeon, M. Engole, N. Abbas, M. Salman Haider, S. J. Kang, H.T. Kim, Sol–gel synthesis of photoactive zirconia–titania from metal salts and investigation of their photocatalytic properties in the photodegradation of methylene blue, Powder Technol. 258 (2014) 99–109, https://doi.org/10.1016/j.powtec.2014.03.024.
[185] R. Shang, A. Goulas, C.Y. Tang, X. de Frias Serra, L.C. Rietveld, S.G.J. Heijman, Atmospheric pressure atomic layer deposition for tight ceramic nanofiltration membranes: synthesis and application in water purification, J. Membr. Sci. 528 (2017) 163–170, https://doi.org/10.1016/j.memsci.2017.01.023.
[186] M. Weber, A. Julbe, A. Ayral, P. Miele, M. Bechelany, Atomic layer deposition for membranes: basics, challenges, and opportunities, Chem. Mater. 30 (2018) 7368–7390, https://doi.org/10.1021/acs.chemmater.8b02687.
[187] S.M. George, Atomic layer deposition: an overview, Chem. Rev. 110 (2010) 111–131, https://doi.org/10.1021/cr900056b.
[188] F. Li, Y. Yang, Y. Fan, W. Xing, Y. Wang, Modification of ceramic membranes for pore structure tailoring: the atomic layer deposition route, J. Membr. Sci. (2012) 17–23, https://doi.org/10.1016/j.memsci.2012.01.005, 397–398.
[189] H. Chen, X. Jia, M. Wei, Y. Wang, Ceramic tubular nanofiltration membranes with tunable performances by atomic layer deposition and calcination, J. Membr. Sci. 528 (2017) 95–102, https://doi.org/10.1016/j.memsci.2017.01.020.
[190] Z. Song, M. Fathizadeh, Y. Huang, K.H. Chu, Y. Yoon, L. Wang, W.L. Xu, M. Yu, TiO2 nanofiltration membranes prepared by molecular layer deposition for water purification, J. Membr. Sci. 510 (2016) 72–78, https://doi.org/10.1016/j.memsci.2016.03.011.
[191] J. Multia, M. Karppinen, Atomic/molecular layer deposition for designer's functional metal–organic materials, Adv. Mater. Interfac. 9 (2022), 2200210, https://doi.org/10.1002/admi.202200210.
[192] S. Chaudhury, E. Wormser, Y. Harari, E. Edri, O. Nir, Tuning the ion-selectivity of thin-film composite nanofiltration membranes by molecular layer deposition of alucone, ACS Appl. Mater. Interfaces 12 (2020) 53356–53364, https://doi.org/10.1021/acsami.0c16569.
[193] R.G. Closser, D.S. Bergsman, S.F. Bent, Molecular layer deposition of a highly stable silicon oxycarbide thin film using an organic chlorosilane and water, ACS Appl. Mater. Interfaces 10 (2018) 24266–24274, https://doi.org/10.1021/acsami.8b06057.

[194] P. Sundberg, M. Karppinen, Organic and inorganic–organic thin film structures by molecular layer deposition: a review, Beilstein J. Nanotechnol. 5 (2014) 1104–1136, https://doi.org/10.3762/bjnano.5.123.
[195] M.A. Cameron, I.P. Gartland, J.A. Smith, S.F. Diaz, S.M. George, Atomic layer deposition of SiO 2 and TiO 2 in alumina tubular membranes: pore reduction and effect of surface species on gas transport, Langmuir 16 (2000) 7435–7444, https://doi.org/10.1021/la9916981.
[196] P.O. Oviroh, R. Akbarzadeh, D. Pan, R.A.M. Coetzee, T.-C. Jen, New development of atomic layer deposition: processes, methods and applications, Sci. Technol. Adv. Mater. 20 (2019) 465–496, https://doi.org/10.1080/14686996.2019.1599694.
[197] S.M. George, B. Yoon, A.A. Dameron, Surface chemistry for molecular layer deposition of organic and hybrid Organic−Inorganic polymers, Acc. Chem. Res. 42 (2009) 498–508, https://doi.org/10.1021/ar800105q.
[198] A.A. Dameron, D. Seghete, B.B. Burton, S.D. Davidson, A.S. Cavanagh, J. A. Bertrand, S.M. George, Molecular layer deposition of alucone polymer films using trimethylaluminum and ethylene glycol, Chem. Mater. 20 (2008) 3315–3326, https://doi.org/10.1021/cm7032977.
[199] S.M. George, B.H. Lee, B. Yoon, A.I. Abdulagatov, R.A. Hall, Metalcones: hybrid organic–inorganic films fabricated using atomic and molecular layer deposition techniques, J. Nanosci. Nanotechnol. 11 (2011) 7948–7955, https://doi.org/10.1166/jnn.2011.5034.
[200] M. Rogowska, P.-A. Hansen, H.H. Sønsteby, J. Dziadkowiec, H. Valen, O. Nilsen, Molecular layer deposition of photoactive metal-naphthalene hybrid thin films, Dalton Trans. 50 (2021) 12896–12905, https://doi.org/10.1039/D1DT02201F.